Published in final edited form as:
Clin Radiol. 2013 June ; 68(6): e275–e290. doi:10.1016/j.crad.2013.01.013.

New era of radiotherapy: an update in radiation-induced lung disease

M. F. K. Benveniste[a,*], **J. Welsh**[b], **M. C. B. Godoy**[a], **S. L. Betancourt**[a], **O. R Mawlawi**[c], and **R. F. Munden**[a]

[a]Department of Diagnostic Radiology, M.D. Anderson Cancer Center, Houston, Texas

[b]Department of Imaging Physics, M.D. Anderson Cancer Center, Houston, Texas

[c]Department of Radiation Oncology, M. D. Anderson Cancer Center, Houston, Texas

Abstract

Over the last few decades, advances in radiotherapy (RT) technology have improved delivery of radiation therapy dramatically. Advances in treatment planning with the development of image-guided radiotherapy and in techniques such as proton therapy, allows the radiation therapist to direct high doses of radiation to the tumour. These advancements result in improved local regional control while reducing potentially damaging dosage to surrounding normal tissues. It is important for radiologists to be aware of the radiological findings from these advances in order to differentiate expected radiation-induced lung injury (RILD) from recurrence, infection, and other lung diseases. In order to understand these changes and correlate them with imaging, the radiologist should have access to the radiation therapy treatment plans.

INTRODUCTION

Radiotherapy (RT) plays a central role in the management of thoracic malignancies including lung, oesophageal and breast neoplasms as well as thymic epithelial neoplasm, malignant pleural mesothelioma and lymphoma. Different RT techniques have been used to plan and deliver radiation to the tumour including three-dimensional (3D) conformal RT (CRT), intensity-modulated RT (IMRT), and stereotactic body RT (SBRT). One of the many challenges of RT in thoracic neoplasms is directing the radiation dose to the target due to tumour motion and anatomical change during treatment. More sophisticated RT technologies, such as four-dimensional (4D) imaging permit an improvement in the therapeutic goals of RT allowing the design of personalized treatment planning that delivers adequate doses directed at the target while sparing the surrounding critical normal tissues (1). More recent advances of proton therapy in thoracic oncology have the potential to achieve higher target doses while improving sparing of normal tissues compared to 3D-CRT or IMRT (2). With these advances in radiation imaging and treatment planning, there are efforts to escalate treatment dosages in hopes of improving local control. The result in escalating doses may lead to changes of the normal patterns of radiation-induced lung

[*]Guarantor and correspondent: M. Benveniste, Department of Diagnostic Radiology, Unit 1478, The University of Texas M. D. Anderson Cancer Center, 1515 Holcombe Blvd, Houston, TX 77030, USA. Tel.: +1 713-745-5149; fax: +1 713-563-0638. mfbenveniste@mdanderson.org.

disease (RILD); therefore, it is essential that radiologists understand these newer techniques and the impact of RILD.

This manuscript will describe the newer methods of planning and delivering RT along with the alterations of traditional patterns of RILD to facilitate radiologist's understanding of these alterations.

BACKGROUND

Ionizing radiation, used in RT, can be caused by electromagnetic or photon radiation (x-ray and gamma-ray), as well as particulate radiation (alpha, neutron, proton and electron). Ionizing radiation causes electron ejection in its target, which loses its energy to the medium in a scale correspondent to LET (linear energy transfer). A low-speed particle with multiple charges has a high LET. In this regard, x-ray and gamma-rays are considered low-LET ionizing radiation compared with proton and alpha particles, which are considered high LET radiation. Ions radicals produced in photon radiation decay rapidly, leading to production of free radicals, which mediate cell damage. The mechanism for cell injury by high LET radiation is direct DNA damage and not free radical formation. High LET transfer cause more biological damage. Radiation-induced injury to cells always starts within milliseconds with chemical changes at the atomic and molecular level. The critical target of radiation is the DNA and cell membrane. Cellular effects range from acute cell death to defective reproduction or reduced functional work. Usually, small doses may produce mitotic damage, whereas larger doses are required for early cell death. Although injury takes place at the time of radiation exposure, clinical expression of the injury may never occur if damage is not extensive or may be expressed weeks, months, or even years after the event.

TREATMENT TERMINOLOGY AND RT PLANNING

Target volume delineation is essential to deliver a high precision radiation dose to the tumour; particularly in lung cancer because the tumour may move outside the treatment field during respiration. Therefore, appropriate margins are added to the treatment field to take respiratory motion into consideration. Radiologists should be aware of the nomenclature for RT treatment plans in order to understand the treatment process. According to guidelines of the International Commission on Radiation Units and Measurements reports (ICRU), different volumes should be prescribed prior to RT (3). The gross tumour volume (GTV) is obtained by outlining the margins of the visible tumour. The clinical target volume (CTV) is an oncological concept and represents the possible presence of microscopic subclinical disease around the lesion. The internal target volume (ITV) is defined as the union of target motion and GTV and accounts for possible tumour movement during treatment, in particular, due to patient's respiration. Finally, the planning target volume (PTV) accounts for set-up uncertainties and represents the effective and global treatment plan.

DOSE AND FRACTIONATION

Different biological parameters influence the response of tissues to RT and the ability to recover from sub-lethal damage is proportional to dose rates and time. Increasing cell death occurs by increasing the dose and/or decreasing the time interval between radiation delivery (fraction). Normal tissues tend to repair faster than tumour cells and, therefore, fractionating the treatment dosages is beneficial for re-population of normal tissues. Additionally, fractionation allows tumour cells in a radioresistant phase of the biological cycle cell (S phase or DNA synthesis) to move to a more radiosensitive phase (M or mitotic phase). Likewise, hypoxic tumour cells that are radioresistant may re-oxygenate between fractions, and become radiosensitive (4). However, fractionation may allow some tumour cells to

repair or even some normal cells to become more sensitive and counteract the beneficial aspects of fractionation (5).

External-beam RT in combination with concurrent platinum-based chemotherapy represents an established treatment option for patients with unresectable locally advanced non-small cell lung cancer (NSCLC; stage III). A standard dose of 60 Gy, given in a single fraction per day, 5 days a week, during 6 weeks was set by the Radiation Therapy Oncology Group (RTOG) 73-01 study based on improved local control and improved survival compared with lower total doses of 40 or 50 Gy given at 2 Gy per fraction (6). Subsequently, other fractionation schedules are occasionally employed in unique situations, such as hyperfractionation in small cell lung cancer and hypofractionation for stage I/II NSCLC where stereotactic approaches are employed (7). In hyperfractionation there is delivery of more than one fraction in 24 h employing a dose per fraction of less than 1.8 Gy (8). In hypofractionation there is delivery of a larger dose per fraction in fewer fractions, with a dose per fraction exceeding 2.2 Gy, which is the basis of stereotactic body radiotherapy. Accelerated fractionation refers to the intensity of the treatment over time in which the rate of dose accumulation exceeds 10 Gy per week. One type of accelerated RT is called continuous hyperfractionated accelerated RT (CHART), which combines hyperfractionation and accelerated schemes in a 54 Gy treatment, given in three fractions a day, 1.5 Gy/day, for 12 days. Saunders and colleagues (9) compared the CHART scheme with standard RT and demonstrated improved survival in NSCLC patients. Yet despite the encouraging data regarding CHART, it has not been adopted in most parts of the world because randomized trials have not shown a significant advantage when compared with conventional fractionated treatment(10).

TREATMENT PLANNING IN THORACIC MALIGNANCIES

RT plays a central role in the management of NSCLC (Fig. 1a – b), and remains the only non-surgical way of curing lung cancer. Although surgical resection remains the standard and curative modality for the treatment of early-stage disease (stage I/II), definitive RT is utilized in patients who are poor surgical candidates. Additionally, multimodality therapy, including RT, is useful in patients with locally advanced NSCLC. In these cases, the treatment plan involves the primary tumour and involved lymph nodes with associated treatment plan margins (11). The patterns of RILD may be different than anticipated because of this extended coverage.

Small-cell lung cancer is classically a chemosensitive tumour. Unfortunately 80% of patients treated with chemotherapy may develop recurrent tumour. RT in limited-stage small-cell disease is used to improve the local tumour control rate and patient survival, and is actually shown to be superior to surgery (12–14). Radiation treatment portals include the primary tumour and involved lymph nodes but may be extended to cover supraclavicular, hilar, and mediastinal regions, resulting in multiple sites of RILD.

In patients with oesophageal cancer, treatment often consists of multimodality therapy either after chemotherapy or in conjunction as chemoradiotherapy. Radiation alone may be a viable option for patients with inoperable cancers who cannot tolerate chemotherapy. Additionally, RT has been used as an adjuvant postoperative treatment in locally advanced disease. The planning tumour volume is focused to the tumour, including a 5–6 cm margin above and below the target to encompass the high-risk lymphatics (Fig. 1c – d) (15). It is important to understand that protection of the spinal cord from radiation is critical to the radiation oncologist, and therefore, the radiation beams are angled, sometimes in various orientations to reduce radiation damage to the spinal cord.

Head and neck planning radiation fields commonly involve the apical aspects of the lungs and result in symmetrical or asymmetrical opacities. These should not be misinterpreted as infectious process.

A combination of breast conservation surgery, sentinel lymph node biopsy, or axillary lymph node dissection and RT has become the standard of care for early-stage breast cancer (16). Treatment plans for breast radiation uses tangential beams to minimize damage to the underlying lung. Typical findings are detected at computed tomography (CT) as parenchymal opacities in the anterolateral aspect of the lung. Treatment may also include coverage of the supraclavicular and internal mammary lymph nodes and will result in apical and paramediastinal opacities, respectively (Fig. 1e – f).

RT has been used as an adjuvant treatment after surgery in patients with locally advanced thymoma as well as in incomplete tumour resection (17), and as neoadjuvant therapy in patients with advanced-stage disease and unresectable tumours.

Patients with malignant pleural mesothelioma have been treated with IMRT after extrapleural pneumonectomy (18, 19). The treatment plan includes all of the pleural space including the extension along the upper abdomen. The outer border of the liver will be included in the treatment field and may produce an unusual pattern that should not be confused with metastatic involvement (Fig. 1g – h) (20).

Lymphoma, including Hodgkin's and non-Hodgkin's disease, is a radiosensitive tumour. Treatment planning includes all lymph nodes compartments above and below the diaphragm with typical broad radiation lung damage of the apex and paramediastinal regions (21, 22).

PATHOPHYSIOLOGY AND CLINICAL FINDINGS

RILD has been classically described as having two phases; an acute phase and chronic phase with the time interval to describe RILD calculated from the date of completion of RT (23). The acute phase, referred to as pneumonitis, occurs 4–12 weeks after treatment is completed (24–26) and the chronic phase, referred to as fibrosis, occurs several months after treatment is completed and may progress slowly for months to years.

Capillary and epithelial cells are more susceptible to damage, and therefore, the acute phases of pneumonitis are typically characterized by injury to small vessels and capillaries with the development of vascular congestion and increased capillary permeability. Other findings in pneumonitis include thickening of the alveolar–capillary space, exudation of proteinaceous material into alveoli, infiltration of inflammatory cells and desquamation of epithelial cells, which result in impairment of gas exchange. If the radiation injury is mild, these changes may resolve. However, when the injury is severe, chronic changes of fibrosis will develop. The histopathological appearance of fibrosis is dominated by fibroblasts proliferation, progressive alveolar septal thickening, and progressive vascular sclerosis. Infrequently, radiation damage can be manifested as organizing pneumonia, most commonly outside the expected radiation field and representing an indirect injury possibly caused by a lymphocyte-mediated hypersensitivity reaction or an immunological disorder (27).

The clinical symptoms of RILD are non-specific and proportional to the total radiation dose, the volume of irradiated lung, and pre-treatment pulmonary function of the patient. If chemotherapy has been added to multimodality treatment, there is an increased risk of clinical symptoms (28, 29). Additional risk factors that may increase the degree of damage include age, cigarette smoking, and pre-existing lung disease. The clinical symptoms are reflective of the histopathological changes. In the acute phase, symptoms occur as early as 1 month after the beginning of RT and as late as 6 months after completion of treatment.

Patients may present with increasing shortness of breath, dry cough, low-grade fever, and chest pain secondary to the capillary leakage and congestion. It is important to note that symptoms may develop before radiological changes. If treatment is needed, steroids, oxygen, and supportive ventilation can be used. An abrupt interruption in steroid treatment also may cause a relapse in acute pneumonitis. If the lung injury progresses, there is development of the late phase of lung damage, represented by pulmonary fibrosis, which typically appears 6 months after the completion of radiotherapy. Patients may be asymptomatic or have variable degree of dyspnoea with severe cases progressing to chronic cor pulmonale due to pulmonary hypertension. Other non-pulmonary effects of radiation damage include oesophagitis, which can be mild to severe and usually worsening toward the end of radiotherapy. Radiation pericarditis usually presents 6–9 months after RT and may present as chest pain. Chronic cardiac abnormalities includes cardiomyopathy and coronary artery disease(24).

USUAL RADIOLOGICAL MANIFESTATIONS OF RADIATION DAMAGE

The radiological appearance of RILD, which is better detected on CT than chest radiographs, correlates with the histopathological features. Even though radiation pneumonitis has been reported to occur with doses as low as 5 Gy(30), in general, lung injury is not seen with doses below 20 Gy (31) and is most commonly seen in patients who have received more than 40 Gy of radiation. Any thoracic tissue exposed to the radiation therapy can develop radiological manifestations of radiation injury.

Acute pneumonitis manifests radiologically as ground-glass opacities or consolidation within the irradiated lung approximately 3–4 weeks after the completion of RT (Fig. 2). Atypical findings are not uncommon and include a crazy-paving pattern (Fig. 3), which refers to fine reticular lung opacities superimposed on areas of ground-glass pattern. In addition, a central ground-glass opacity surrounded by a denser air-space consolidation defined as a reversed halo sign may develop (Fig. 4). Radiation pneumonitis beyond the radiation field is reported to occur, although is not usual (23). The pulmonary opacities of pneumonitis can subside if the lung injury is limited; otherwise the changes progress into those of the fibrotic phase. Radiation fibrosis manifests as consolidation, traction bronchiectasis, architectural distortion, and volume loss that usually develops 6–12 months after RT completion and stabilizes within 2 years (Fig. 5). Other thoracic structures may develop changes due to radiation damage. Pleural effusions are frequently seen on CT around 6 months after therapy (24). If there is a continuous increase in volume of pleural effusion or if it develops after 6 months, a cytological evaluation may be needed to exclude malignancy. Pericardial effusions occur within the first 3 years after therapy (32) and are usually small and self-limited. Oesophagitis can appear as circumferential wall thickening at CT and as a diffuse 2-[18F]-fluoro-2-deoxy-D-glucose (FDG) activity without focal abnormality at positron-emission tomography (PET). Oncological patients treated with high-dose RT may also develop oesophageal stricture (33). Additionally, irradiated muscle included in the spectrum of the radiation beam, may also demonstrate inflammatory changes detected as increased FDG uptake in PET studies (34).

DIFFERENTIAL DIAGNOSIS CONSIDERATIONS

Patients treated with RT usually are followed radiologically to assess for effects of radiation treatment, to exclude recurrent tumour, and to detect superimposed lung disease. Correlation with the radiation treatment plans, the type and course of radiotherapy, and previous imaging studies for temporal correlation are important to correctly interpret the manifestations of radiation damage. When radiological manifestations of radiation damage are different from the expected patterns, it may be from an unusual manifestation of

radiation injury, but other disease entities have to be considered. The most common disease entities to consider in the differential diagnosis are infection and recurrent tumour. The clinical presentation of infection and recurrent tumour may be non-specific and have similarities to the effects of RT, and therefore, the radiological appearance may be useful in differentiating these entities.

Because radiation pneumonitis generally starts 4–6 weeks after the radiation treatment is completed, any lung opacity that occurs before completion of therapy may represent an infectious process. Additionally, as radiation pneumonitis has a more indolent and slowly progressive course than an infectious aetiology, an abrupt onset is suggestive of infection; an exception would be recent discontinuation of steroid therapy(35). Other indications of infection include lung opacities outside of the treated radiation areas (Fig. 6) or development of centrilobular nodules in a tree in bud pattern (15, 35). The development of patchy and migratory lung opacities is suspicious for organizing pneumonia (Fig. 7). Additional criteria for organizing pneumonia diagnosis described in a study for breast cancer patients include: (1) RT within the last 12 months, (2) general and/or respiratory symptoms lasting for at least 2 weeks, (3) discrepancy between the images and the symptoms, and (4) no evidence of a specific cause, such as collagen vascular disease, drug toxicity, or allergic disease(36). The development of cavitation within the radiation fibrosis may indicate an infectious process including tuberculosis, but, unfortunately, post-RT lung necrosis (37) and recurrent tumour may present with cavitation. Finally, one of the most important indications of superimposed disease within the radiation fibrosis is the loss of bronchiectasis due to filling in of the airways. This is usually secondary to infection or recurrent tumour, and thus, may require bronchoscopic evaluation to determine the cause.

Local tumour recurrence usually occurs within 2 years after treatment ends, but it may be difficult to detect radiographically because of the fibrotic changes within the irradiated lung. As noted, filling in of the bronchiectatic airways can be an important indication of tumour recurrence. Another indication of recurrence is an increase in the contour of the radiation fibrosis border or development of a lobulate contour within the fibrosis (Fig. 8). The evaluation for recurrent tumour within radiation fibrosis has been improved with the utilization FDG PET-CT, because PET-CT can differentiate metabolic active tumour from inactive post-radiation fibrosis (Fig. 9). The inflammation of radiation pneumonitis may show increased FDG activity that may persist for months(38), and therefore, PET-CT is best performed 6 months after treatment is completed(35). Even so, low-grade and diffuse FDG activity within the treated lung may persist after radiotherapy, but findings of focal FDG uptake is suggestive of residual or recurrent disease. One study by Bury *et al*. (38) included 126 patients with NSCLC who underwent CT and PET in the assessment of therapeutic effects. In detecting residual or recurrent NSCLC, PET had a sensitivity of 100% and specificity of 92%, whereas CT had a sensitivity and specificity of 71% and 95%, respectively. An additional benefit of PET-CT imaging in post-radiation patients is that the FDG activity can be helpful for guidance in lung biopsy, if needed. Findings of tumour progression other than a change in the fibrosis include lymphangitic spread (nodular interlobular septal thickening, peribronchovascular bundle involvement), new or enlarging hilar/mediastinal lymph nodes and new or enlarging pleural effusion.

NEWER TYPES OF RT DELIVERY AND IMAGING

The main goal for RT planning and delivery is to achieve target delineations that result in high therapeutic tumour doses with minimal toxicity to normal surrounding structures (1). Older treatment technologies, such as two-dimensional (2D) radiation portals coupled with lower energy treatment precluded high-dose treatments and often resulted in local recurrences, especially in patients with NSCLC (39, 40). Improvements in delivery

techniques such as 3D-CRT and IMRT resulted in improved local tumour control because higher doses could be delivered without increasing toxicity (41–43). Modern 3D- CRT uses a 3D image reconstructed from CT scanning data to determine the target volumes to be treated. A computer planning system is used to design beam arrangements with a variety of orientations that deliver maximal radiation dose to the tumour while limiting exposure to normal structures.

When thoracic malignancies are treated with 3D conformal irradiation, RILD can manifest in patterns different than those with older 2D treatment. Patterns have been described as a modified conventional pattern, which shows volume loss, consolidation, and bronchiectasis, similar to, but less extensive than, conventional radiation fibrosis, a scar-like pattern, which accounts for linear opacity in the region of the original tumour, or a mass-like pattern (Fig. 10) (44). Radiation pneumonitis from these newer techniques can manifest as focal consolidative opacities within the treatment port or also as poorly marginated and irregular lung nodules (25, 45) (Fig. 11). In this specific scenario, metastatic disease is excluded as it would be more likely to present outside of the radiation field rather than within the treated lung.

The shape and distribution of lung damage will vary according to the type, location, and extension of primary tumour and the corresponding beam arrangement used to encompass it. An essential aide in understanding radiological manifestations of RILD is to review RT treatment plans with dose distribution lines. The patterns of RILD on imaging should correlate with the treatment fields and dosage, whereas disease outside of the treatment fields likely indicates other entities, such as infection or malignancy. Additionally, as 3D techniques may result in radiation being delivered through thoracic structures other than typically seen in conventional delivery, correlation with treatment plans can prevent radiologist from attributing RILD findings to other diseases. In some cases, there may be RILD findings in ipsilateral or contralateral lobes from the primary tumour or in a geographic orientation away from the site of the primary disease (Fig. 12).

In IMRT the radiation dose distributions are more conformal to the target with a steep fall in the dose to the neighbouring normal tissues (46), thus sparing a large volume of normal tissue and allowing highly accurate target coverage (Fig. 13). Murshed and Liao,[47] in a study of 41 patients with advanced stage NSCLC (stage III–IV) demonstrated a 10% improved target conformity of IMRT when compared to 3D-CRT (47). Unusual patterns may also result from the beam configuration as previously noted.

SBRT is a high-dose radiation treatment used to treat small tumours, especially peripheral early-stage NSCLC (Fig. 14). SBRT utilizes 3D-CRT with multiple non-co-planar beams conformed to the shape of the target. Fewer fractions with higher dose and steep dose gradients are used in this technique. Although early-stage NSCLC is typically managed with surgical resection (48, 49), SBRT has been used in medically inoperable patients with early-stage NSCLC (50) and is shown to have local-control rates comparable to those observed with surgical resection. There is further interest in investigating SBRT versus surgery for NSCLCs because SBRT offers a high local control rates together with a low risk for complications (51, 52), particularly when compared with poor results from conventional RT (39, 40, 53).

NEW TECHNOLOGIES IN RT

Technological advances in RT, such as 4D CT techniques, applications of PET-CT during treatment, and proton therapy, continue to advance the effectiveness and precision in RT delivery. These techniques allow dose escalation to the target while sparing surrounding normal structures (54, 55).

4D–CT techniques improves treatment in image-guided RT (IGRT) by incorporating time into the initial 3D plan to compensate for tumour motion that occurs either during a single fraction (intra-fraction) or between multiple fractions (inter-fractional)(56). In 4D acquisitions, the tumour is gated according to the respiratory cycle in a prospective or retrospective protocol by using respiratory gating or motion-tracking techniques. In lung cancer, utilization of 4D–CT techniques allows high precision radiation therapy (56). In addition to using PET-CT imaging for developing treatment plans, the technique of "dose painting" is being investigated. This involves the application of varying radiation dosage to the tumour based on tumour inhomogeneity identified by FDG imaging. Others are investigating the utility of PET-CT imaging during treatment to detect areas of resistance so that boost doses may be applied to more resistant tumour region(57). Although not established in clinical settings, respiratory gated 4D PET-CT may prove to be helpful for better tumour delineation for RT planning in lung cancers (58).

The physical characteristics of proton therapy results in delivery of a therapeutic dose to a certain depth (as defined by the Bragg peak) with minimal exit doses beyond the tumour. This characteristic provides the ability to direct high-dose radiation delivery to the tumour while avoiding uninvolved critical structures. When retrospectively compared to 3D CRT and IMRT, proton therapy has been shown to significantly reduce the dose delivered to normal lung tissue, the heart, spinal cord, and, in certain cases, the oesophagus. Treatment planning studies suggests that proton RT may have an advantage over conventional photon RT in achieving higher tumour doses and local tumour control with additional improvement in survival with lower toxicity (2, 59, 60). Hoppe *et al*. (61) showed that proton-based RT resulted in lower doses to critical organs at risk and a smaller volume of normal lung exposed to radiation. Currently, proton therapy has been indicated for prior irradiated tumours that need to be irradiated again and for targets that are near at-risk structures such as the mediastinum, heart, oesophagus, and spinal cord (Fig. 15) (62).

Initial proton treatments used passive scatter technology with single-beam energy per field, whereas newer treatments are using scanning beam technology, which divides the beam into many smaller beamlets with variable intensity, referred to as intensity modulated proton therapy (IMPT). However, this technique is clinically limited by tumour motion issues, which frequently require pulmonary gating or anaesthesia to eliminate motion. Efforts are actively underway to address these motion-related uncertainties. It is anticipated that the patterns of RILD from these newer techniques will be similar to but less than those seen in 3D conformal treatment.

CONCLUSION

RT is an important modality in the treatment of patients with thoracic neoplasms. Knowledge of newer radiation techniques is important for the radiologist to recognize patterns of RILD and detect complications, such as recurrent malignancy or infection.

REFERENCES

1. Chang JY, Cox JD. Improving radiation conformality in the treatment of non-small cell lung cancer. Semin Radiat Oncol. 2010; 20:171–177. [PubMed: 20652085]
2. Chang JY, Zhang X, Wang X, et al. Significant reduction of normal tissue dose by proton radiotherapy compared with three-dimensional conformal or intensity-modulated radiation therapy in stage I or stage III non-small-cell lung cancer. Int J Radiat Oncol Biol Phys. 2006; 65:1087–1096. [PubMed: 16682145]
3. International Comission on Radiation Units and Measurements. Prescribing, recording, and reporting photon beam therapy. Bethesda, MDL: ICRUM; 1993.

4. Withers, HR. The four R's of radiotherapy. In: Lett, JT.; Adler, H., editors. Advances in Radiation Biology. New York: Academic Press; 1975. p. 241-271.
5. Timmerman R, Bastasch M, Saha D, Abdulrahman R, Hittson W. Story MOptimizing dose fractionation for stereotactic body radiation therapy Normal tissue and tumor control effects with large dose per fraction. Front Radiat Ther Oncol. 2007; 40:352–365. [PubMed: 17641519]
6. Perez CA, Stanley K, Rubin P, et al. A prospective randomized study of various irradiation doses and fractionation schedules in the treatment of inoperable non-oat-cell carcinoma of the lung Preliminary report by the Radiation Therapy Oncology Group. Cancer. 1980; 45:2744–2753. [PubMed: 6991092]
7. Stuschke M, Pottgen C. Altered fractionation schemes in radiotherapy. Front Radiat Ther Oncol. 42:150–156. [PubMed: 19955801]
8. Ruysscher, DK.; Khoo, VS.; Bentzen, SM. Biological basis of fractionation and timing of radiotherapy. In: Pass, HCDP.; Minna, JD.; Johnson, DH.; Scagliotti, GV.; Turrisi, AT., editors. Principles & Practice of Lung Cancer: The Official Reference Text of the IASLC. 4th edn.. Philadelphia, PA: Lippincott Willians & Wilkins; 2010.
9. Saunders M, Dische S, Barrett A, Harvey A, Griffiths G, Palmar M. Continuous, hyperfractionated, accelerated radiotherapy (CHART) versus conventional radiotherapy in non-small cell lung cancer: mature data from the randomised multicentre trial CHART Steering committee. Radiother Oncol. 1999; 52:137–148. [PubMed: 10577699]
10. Hatton MQ, Martin JE. Continuous hyperfractionated accelerated radiotherapy (CHART) and non-conventionally fractionated radiotherapy in the treatment of non-small cell lung cancer: a review and consideration of future directions. Clin Oncol (R Coll Radiol). 2010; 22:356–364. [PubMed: 20399629]
11. Emami, BG.; Lung, MV. Perez and Brady's Principles and Practice of Radiation Oncology. 3rd edn.. Perez, CA.; Brady, LW., editors. Philadelphia: Lippincott-Raven; 1998.
12. Fox W, Scadding JG. Medical Research Council comparative trial of surgery and radiotherapy for primary treatment of small-celled or oat-celled carcinoma of bronchus. Ten-year follow-up. Lancet. 1973; 2:63–65.
13. Pignon JP, Arriagada R, Ihde DC, et al. A meta-analysis of thoracic radiotherapy for small-cell lung cancer. N Engl J Med. 1992; 327:1618–1624. [PubMed: 1331787]
14. Warde P, Payne D. Does thoracic irradiation improve survival and local control in limited-stage small-cell carcinoma of the lung? A meta-analysis. J Clin Oncol. 1992; 10:890–895. [PubMed: 1316951]
15. Park KJ, Chung JY, Chun MS, Suh JH. Radiation-induced lung disease and the impact of radiation methods on imaging features. RadioGraphics. 2000; 20:83–98. [PubMed: 10682774]
16. Ogo E, Komaki R, Abe T, Uchida M, Fujimoto K, Suzuki G, et al. The clinical characteristics and non-steroidal treatment for radiation-induced bronchiolitis obliterans organizing pneumonia syndrome after breast-conserving therapy. Radiother Oncol. 2010; 97:95–100. [PubMed: 20385415]
17. Benveniste MF, Rosado-de-Christenson ML, Sabloff BS, Moran CA, Swisher SG, Marom EM. Role of imaging in the diagnosis, staging, and treatment of thymoma. RadioGraphics. 2011; 31:1847–1861. discussion 61–3. [PubMed: 22084174]
18. Ahamad A, Stevens CW, Smythe WR, et al. Intensity-modulated radiation therapy: a novel approach to the management of malignant pleural mesothelioma. Int J Radiat Oncol Biol Phys. 2003; 55:768–775. [PubMed: 12573764]
19. Forster KM, Smythe WR, Starkschall G, et al. Intensity-modulated radiotherapy following extrapleural pneumonectomy for the treatment of malignant mesothelioma: clinical implementation. Int J Radiat Oncol Biol Phys. 2003; 55:606–616. [PubMed: 12573747]
20. Iyer RB, Balachandran A, Bruzzi JF, Johnson V, Macapinlac HA, Munden RF. PET/CT and hepatic radiation injury in esophageal cancer patients. Cancer Imaging. 2007; 7:189–194. [PubMed: 18055293]
21. Gospodarowicz, MKWTH. Non-Hodgkin's Lymphoma. 3rd ed.. Perez, CABLW., editor. Philadelphia: Lippincott-Raven; 1998.

22. Hoppe, RT. Hodgkin`s Disease. 3rd ed.. Perez, CABLW., editor. Philadelphia: Lippincott-Raven; 1998.
23. Choi YW, Munden RF, Erasmus JJ, et al. Effects of radiation therapy on the lung: radiologic appearances and differential diagnosis. RadioGraphics. 2004; 24:985–997. discussion 98. [PubMed: 15256622]
24. Libshitz HI, Dubrow RA, Loyer EM, Charnsangajev C. Radiation change in normal organs: an overview of body imaging. Eur radiol. 1996; 6:786–795. [PubMed: 8972312]
25. Libshitz HI, Shuman LS. Radiation-induced pulmonary change: CT findings. J Comput Assist Tomogr. 1984 Feb.8:15–19. [PubMed: 6690504]
26. Davis SD, Yankelevitz DF, Henschke CI. Radiation effects on the lung: clinical features, pathology, and imaging findings. AJR Am J Roentgenol. 1992; 159:1157–1164. [PubMed: 1442375]
27. Guerriero G, Battista C, Montesano M, et al. Unusual complication after radiotherapy for breast cancer bronchiolitis obliterans organizing pneumonia case report and review of the literature. Tumori. 2005; 91:421–423. [PubMed: 16459640]
28. Graham MV, Pajak TE, Herskovic AM, Emami B, Perez CA. Phase I/II study of treatment of locally advanced (T3/T4) non-oat cell lung cancer with concomitant boost radiotherapy by the Radiation Therapy Oncology Group (RTOG 83–12): long-term results. Int J Radiat Oncol Biol Phys. 1995; 31:819–825. [PubMed: 7860394]
29. Liao ZX, Travis EL, Tucker SL. Damage and morbidity from pneumonitis after irradiation of partial volumes of mouse lung. Int J Radiat Oncol Biol Phys. 1995; 32:1359–1370. [PubMed: 7635776]
30. Wang S, Liao Z, Wei X, Liu HH, Tucker SL, Hu CS, et al. Analysis of clinical and dosimetric factors associated with treatment-related pneumonitis (TRP) in patients with non-small-cell lung cancer (NSCLC) treated with concurrent chemotherapy and three-dimensional conformal radiotherapy (3D-CRT). Int J Radiat Oncol Biol Phys. 2006; 66:1399–1407. [PubMed: 16997503]
31. Jennings FLAA. Development of radiation pneumonitis: time and dose factor. Arch Pathol. 1962; 74:351–360. [PubMed: 14041927]
32. Mill WB, Baglan RJ, Kurichety P, Prasad S, Lee JY, Moller R. Symptomatic radiation-induced pericarditis in Hodgkin's disease. Int J Radiat Oncol Biol Phys. 1984; 10:2061–2065. [PubMed: 6436206]
33. Marks LZJ, Light K. Radiation-induced esophageal stricture following therapy for lung cancer Its clinical course and analysis comparing stricture lenght with isodose levels. Int J Radiat Oncol Biol Phys. 2006; 66:S66–S67.
34. Reinhardt MJ, Kubota K, Yamada S, Iwata R, Yaegashi H. Assessment of cancer recurrence in residual tumors after fractionated radiotherapy: a comparison of fluorodeoxyglucose, L-methionine and thymidine. J Nucl Med. 1997; 38:280–287. [PubMed: 9025756]
35. Erasmus, JJBMK.; Munden, RF. Radiation-Induced Lung Disease. 1st edn.. Muller, NLSCIS., editor. Philadelphia: Saunders-Elsevier; 2008.
36. Crestani B, Valeyre D, Roden S, Wallaert B, Dalphin JC, Cordier JF. Bronchiolitis obliterans organizing pneumonia syndrome primed by radiation therapy to the breast The Groupe d'Etudes et de Recherche sur les Maladies Orphelines Pulmonaires (GERM”O”P). Am J Respir Crit Care Med. 1998; 158:1929–1935. [PubMed: 9847288]
37. Mesurolle B, Qanadli SD, Merad M, et al. Unusual radiologic findings in the thorax after radiation therapy. RadioGraphics. 2000; 20:67–81. [PubMed: 10682772]
38. Bury T, Corhay JL, Duysinx B, et al. Value of FDG-PET in detecting residual or recurrent nonsmall cell lung cancer. Eur Respir J. 1999; 14:1376–1380. [PubMed: 10624770]
39. Armstrong JG, Minsky BD. Radiation therapy for medically inoperable stage I and II non-small cell lung cancer. Cancer Treat Rev. 1989; 16:247–255. [PubMed: 2561593]
40. Coy P, Kennelly GM. The role of curative radiotherapy in the treatment of lung cancer. Cancer. 1980; 45:698–702. [PubMed: 6244073]
41. Fang LC, Komaki R, Allen P, Guerrero T, Mohan R, Cox JD. Comparison of outcomes for patients with medically inoperable stage I non-small-cell lung cancer treated with two-dimensional vs.

three-dimensional radiotherapy. Int J Radiat Oncol Biol Phys. 2006 Sep 1.66:108–116. [PubMed: 16904517]

42. Bradley JD, Ieumwananonthachai N, Purdy JA, et al. Gross tumor volume, critical prognostic factor in patients treated with three-dimensional conformal radiation therapy for non-small-cell lung carcinoma. Int J Radiat Oncol Biol Phys. 2002; 52:49–57. [PubMed: 11777621]
43. Rosenzweig KE, Fox JL, Yorke E, et al. Results of a phase I dose-escalation study using three-dimensional conformal radiotherapy in the treatment of inoperable nonsmall cell lung carcinoma. Cancer. 2005; 103:2118–2127. [PubMed: 15830346]
44. Koenig TR, Munden RF, Erasmus JJ, et al. Radiation injury of the lung after three-dimensional conformal radiation therapy. AJR Am J Roentgenol. 2002; 178:1383–1388. [PubMed: 12034601]
45. Pagani JJ, Libshitz HI. CT manifestations of radiation-induced change in chest tissue. J Comput Assist Tomogr. 1982; 6:243–248. [PubMed: 7076916]
46. Staffurth J. A review of the clinical evidence for intensity-modulated radiotherapy. Clin Oncol (R Coll Radiol). 2010; 22:643–657. [PubMed: 20673708]
47. Murshed HLHH, Liao Z. Dose and volume reduction for normal lung using intensity-modulated radiotherapy for advanced-stage non-small-cell lung cancer. Int J Radiat Oncol Biol Phys. 2004; 58:1258–1267. [PubMed: 15001271]
48. Mountain CF. A new international staging system for lung cancer. Chest. 1986; 89:225S–233S. [PubMed: 3514171]
49. Shields TW. Surgical therapy for carcinoma of the lung. Clin Chest Med. 1993; 14:121–147. [PubMed: 8384959]
50. Onishi H, Shirato H, Nagata Y, et al. Hypofractionated stereotactic radiotherapy (HypoFXSRT) for stage I non-small cell lung cancer: updated results of 257 patients in a Japanese multi-institutional study. J Thorac Oncol. 2007; 2(Suppl. 3):S94–s100. [PubMed: 17603311]
51. Baumann P, Nyman J, Hoyer M, et al. Stereotactic body radiotherapy for medically inoperable patients with stage I non-small cell lung cancer - a first report of toxicity related to COPD/CVD in a non-randomized prospective phase II study. Radiother Oncol. 2008; 88:359–367. [PubMed: 18768228]
52. Hoyer M, Roed H, Traberg Hansen A, et al. Phase II study on stereotactic body radiotherapy of colorectal metastases. Acta Oncol. 2006; 45:823–830. [PubMed: 16982546]
53. Hafty BGGNB, Gerstley J. Results of radical radiation therapy in clinical stage I, technically inoperable non-small-cell lung cancer. Int J Radiat Oncol Biol Phys. 1988; 15:69–73. [PubMed: 2839443]
54. Mancosu P, Bettinardi V, Passoni P, et al. Contrast enhanced 4D–CT imaging for target volume definition in pancreatic ductal adenocarcinoma. Radiother Oncol. 2008; 87:339–342. [PubMed: 18486253]
55. Rietzel E, Liu AK, Doppke KP, et al. Design of 4D treatment planning target volumes. Int J Radiat Oncol Biol Phys. 2006; 66:287–295. [PubMed: 16904528]
56. Li G, Citrin D, Camphausen K, et al. Advances in 4D medical imaging and 4D radiation therapy. Technol Cancer Res Treat. 2008; 7:67–81. [PubMed: 18198927]
57. Feng M, Kong FM, Gross M, Fernando S, Hayman JA, Ten Haken RK. Using fluorodeoxyglucose positron emission tomography to assess tumor volume during radiotherapy for non-small-cell lung cancer and its potential impact on adaptive dose escalation and normal tissue sparing. Int J Radiat Oncol Biol Phys. 2009; 73:1228–1234. [PubMed: 19251094]
58. Bettinardi V, Picchio M, Di Muzio N, Gianolli L, Gilardi MC, Messa C. Detection and compensation of organ/lesion motion using 4D–PET/CT respiratory gated acquisition techniques. Radiother Oncol. 2010; 96:311–316. [PubMed: 20708809]
59. Chang JY, Komaki R, Wen HY, et al. Toxicity and patterns of failure of adaptive/ablative proton therapy for early-stage, medically inoperable non-small cell lung cancer. Int J Radiat Oncol Biol Phys. 2011; 80:1350–1357. [PubMed: 21251767]
60. Auberger T, Seydl K, Futschek T, Sztankay A, Sweeney RA, Lukas P. Photons or protons: precision radiotherapy of lung cancer. Strahlenther Onkol. 2007; 183 Spec No 2:3–6. [PubMed: 18166995]

61. Hoppe BS, Huh S, Flampouri S, et al. Double-scattered proton-based stereotactic body radiotherapy for stage I lung cancer: a dosimetric comparison with photon-based stereotactic body radiotherapy. Radiother Oncol. 97:425–430. [PubMed: 20934768]

62. Hoppe BS, Flampouri S, Li Z, Mendenhall NP. Cardiac sparing with proton therapy in consolidative radiation therapy for Hodgkin lymphoma. Leuk Lymphoma. 51:1559–1562. [PubMed: 20578823]

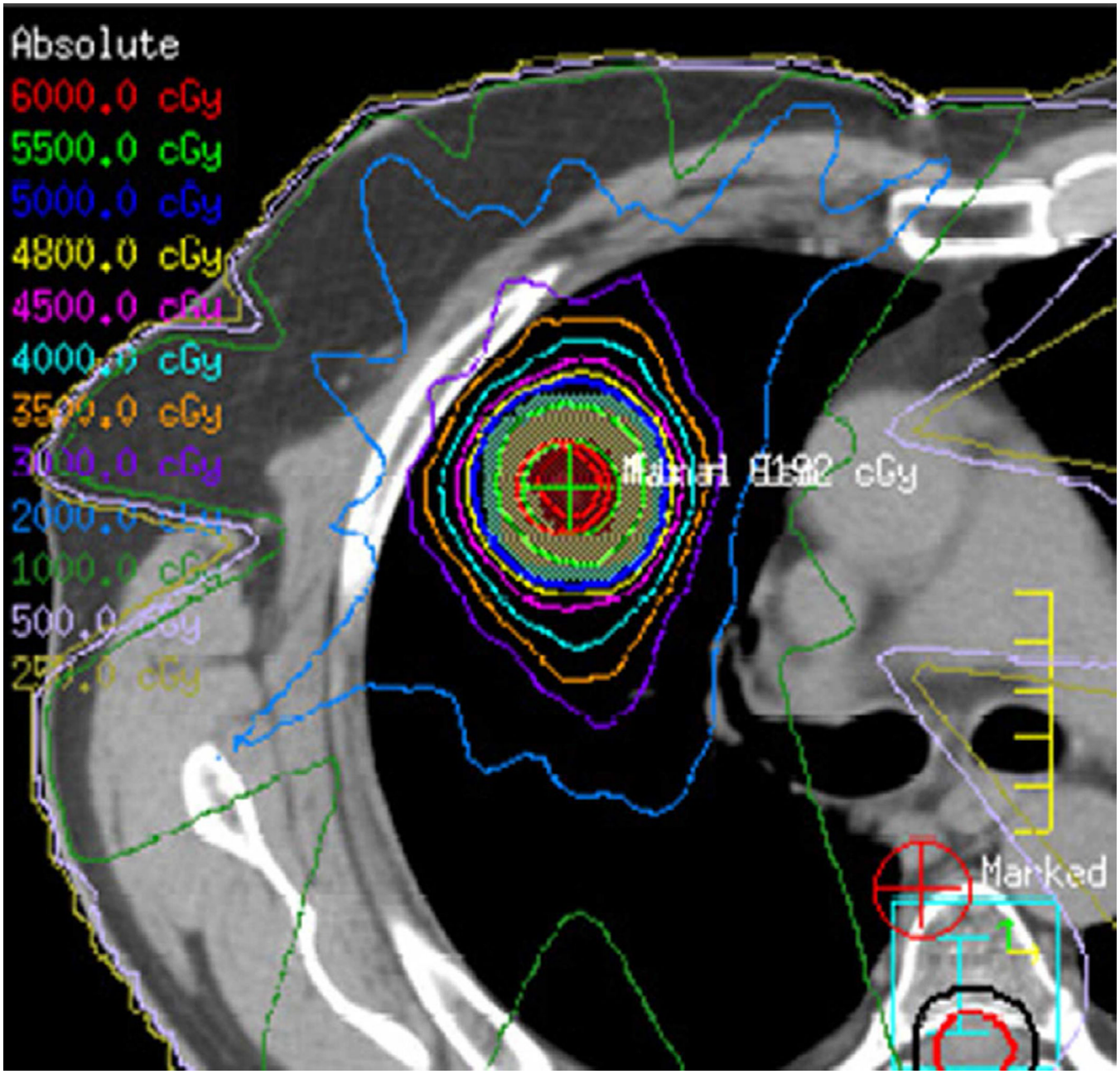

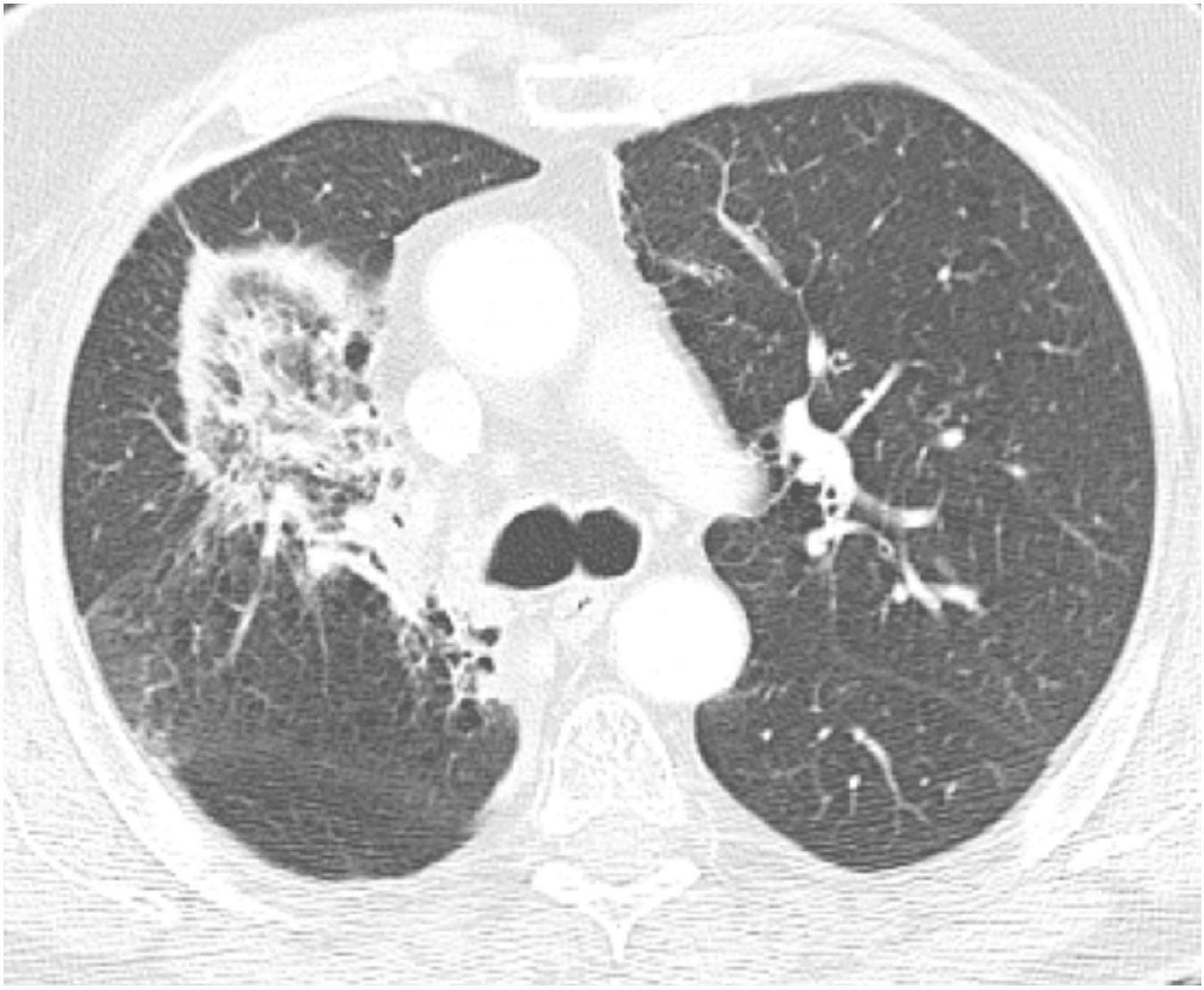

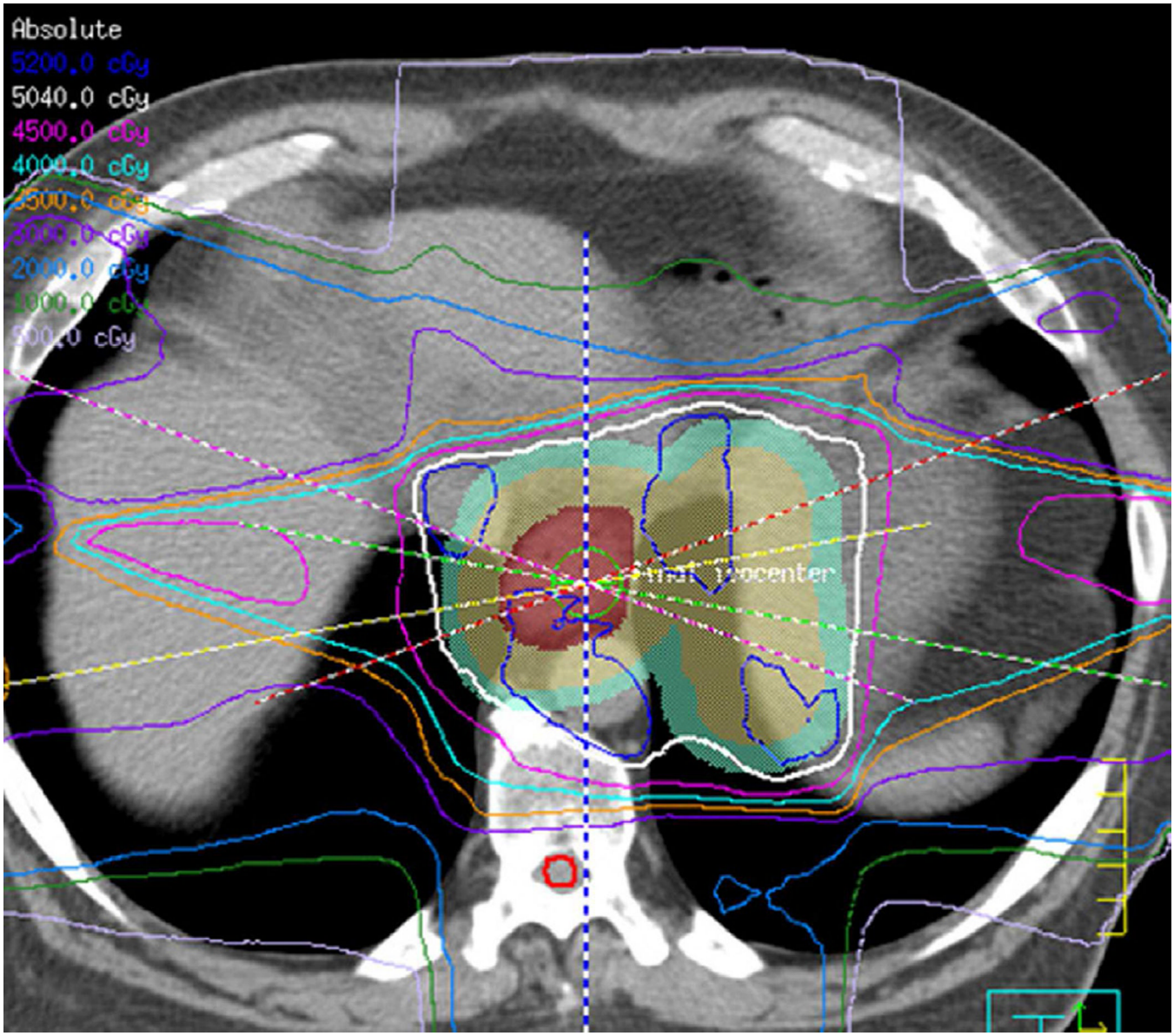

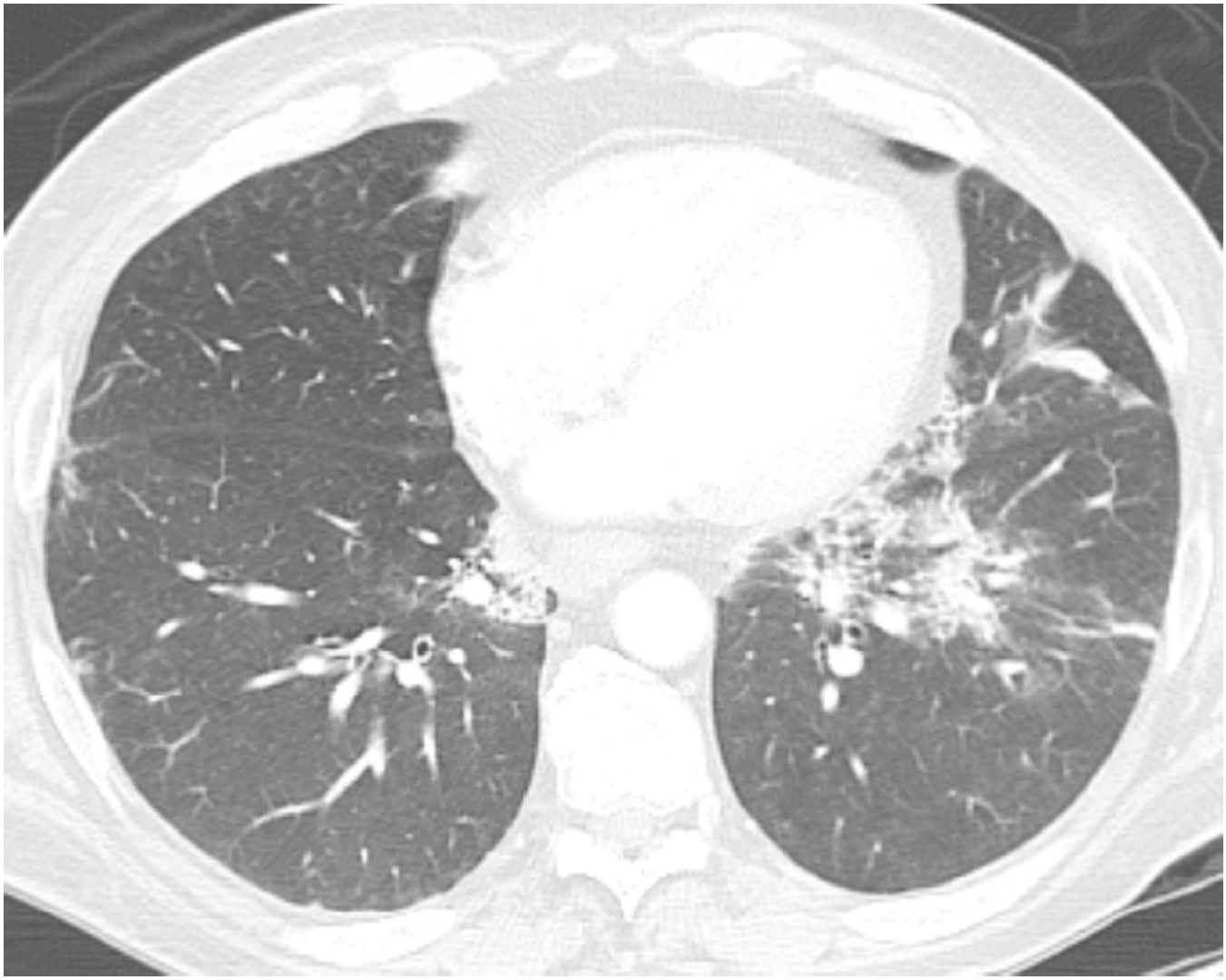

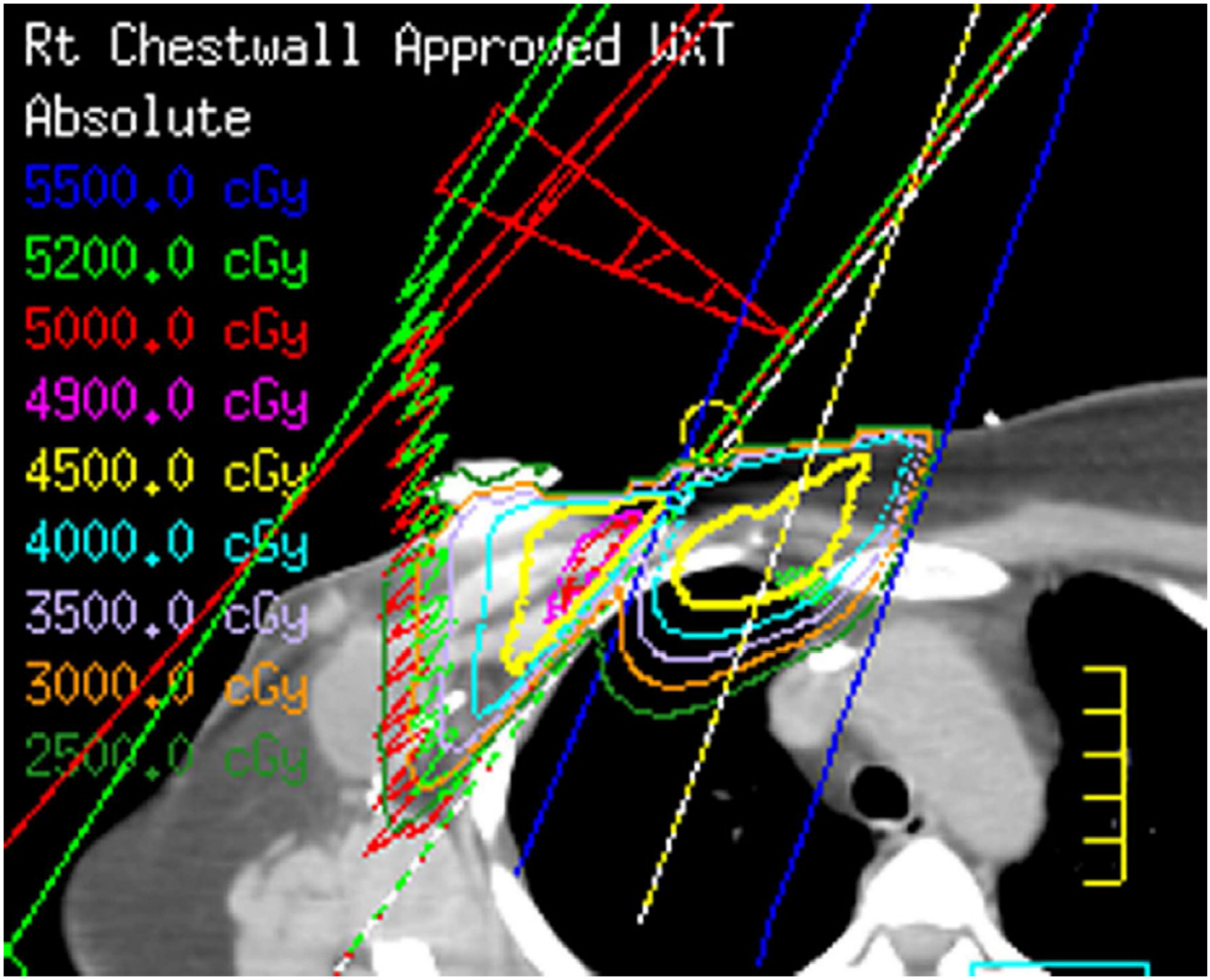

Fig. 1. Planning treatment fields in different intra thoracic malignancies

(a) Patient with NSCLC with IMRT focused in the primary lung malignancy. A Total dose of 63 Gy in 27 fractions was delivered.

(b) Axial CT image obtained 4 months after completion of therapy shows left lung opacities included in the treatment planning field consistent with radiation pneumonitis.

(c) Patient with oesophageal malignancy extending to the gastro-oesophageal junction. IMRT permit a focused treatment to the oesophagus and positive loco-regional lymph nodes while sparing spinal cord, heart, and mediastinum. A total dose of 50.4 Gy in 28 fractions was delivered.

(d) Axial CT image obtained 3 months after treatment ending in a patient with oesophageal malignancy demonstrates lung opacities in the lower lobes included in the irradiated field.

(e) Patient with breast cancer treated with 3D-CRT including right lateral chest wall, supraclavicular and internal mammary regions treated with a total dose of 50 Gy in 25 fractions.

(f) Axial CT image obtained 4 months after completion of therapy shows right apical lung opacities consistent with radiation pneumonitis. Treatment planning field is helpful to differentiate radiation lung injury from an infectious process.

(g) Patient with malignant pleural mesothelioma located in the right side. Patient received surgical treatment with extrapleural pneumonectomy and was treated with postoperative

radiotherapy. Treatment was delivered to the right thoracic cavity with a total dose of 50 Gy in 25 fractions. Note that treatment planning included the dome of the liver.
(h) Axial CT image after administration of intravenous contrast medium obtained 4 months after completion of therapy shows surgical changes due to right extrapleural pneumonectomy and signs of resection/reconstruction of the right hemidiaphragm. Peripheral band of low attenuation (arrows) is seen in the right lobe of the liver which is consistent with post radiation changes.

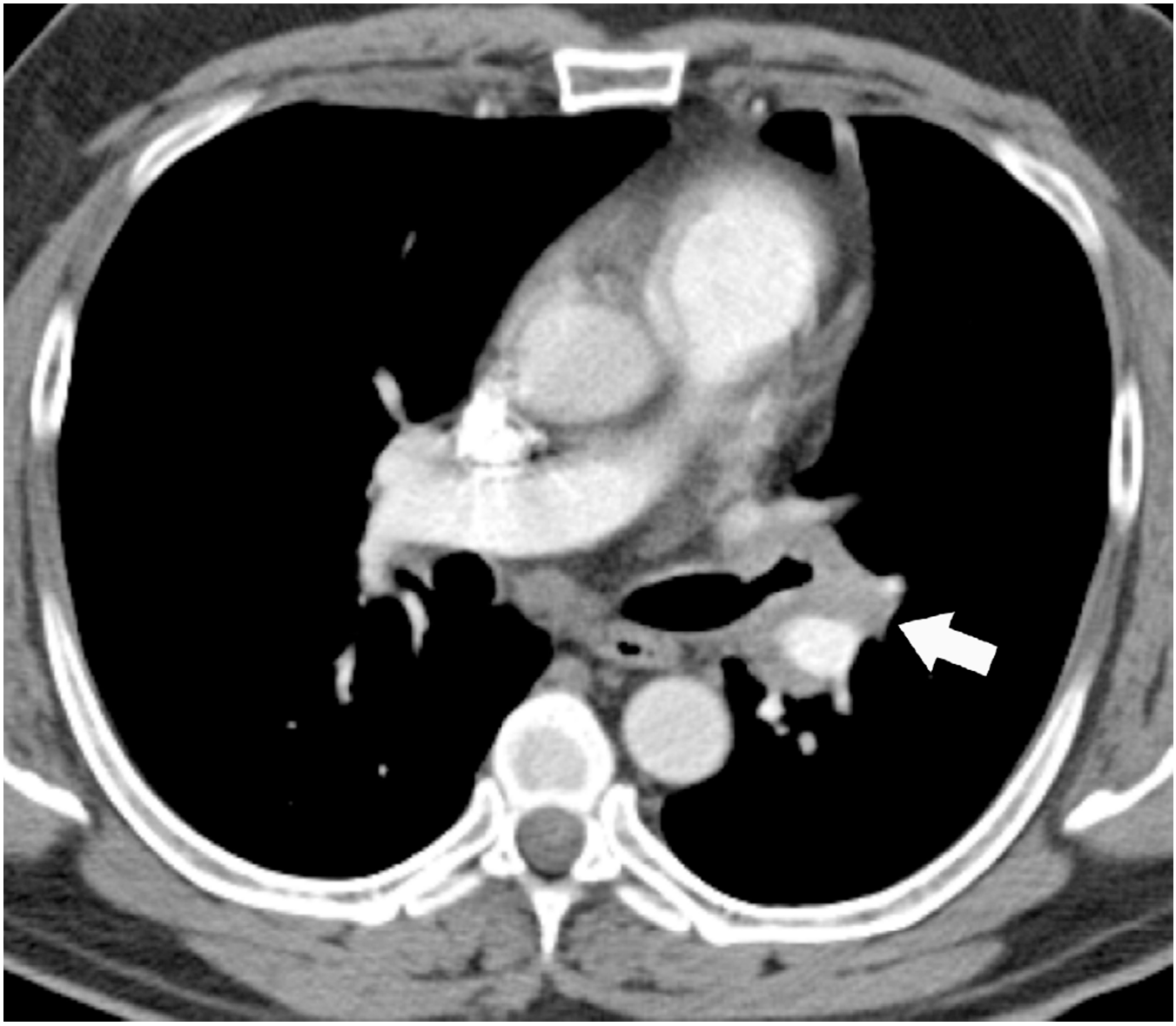

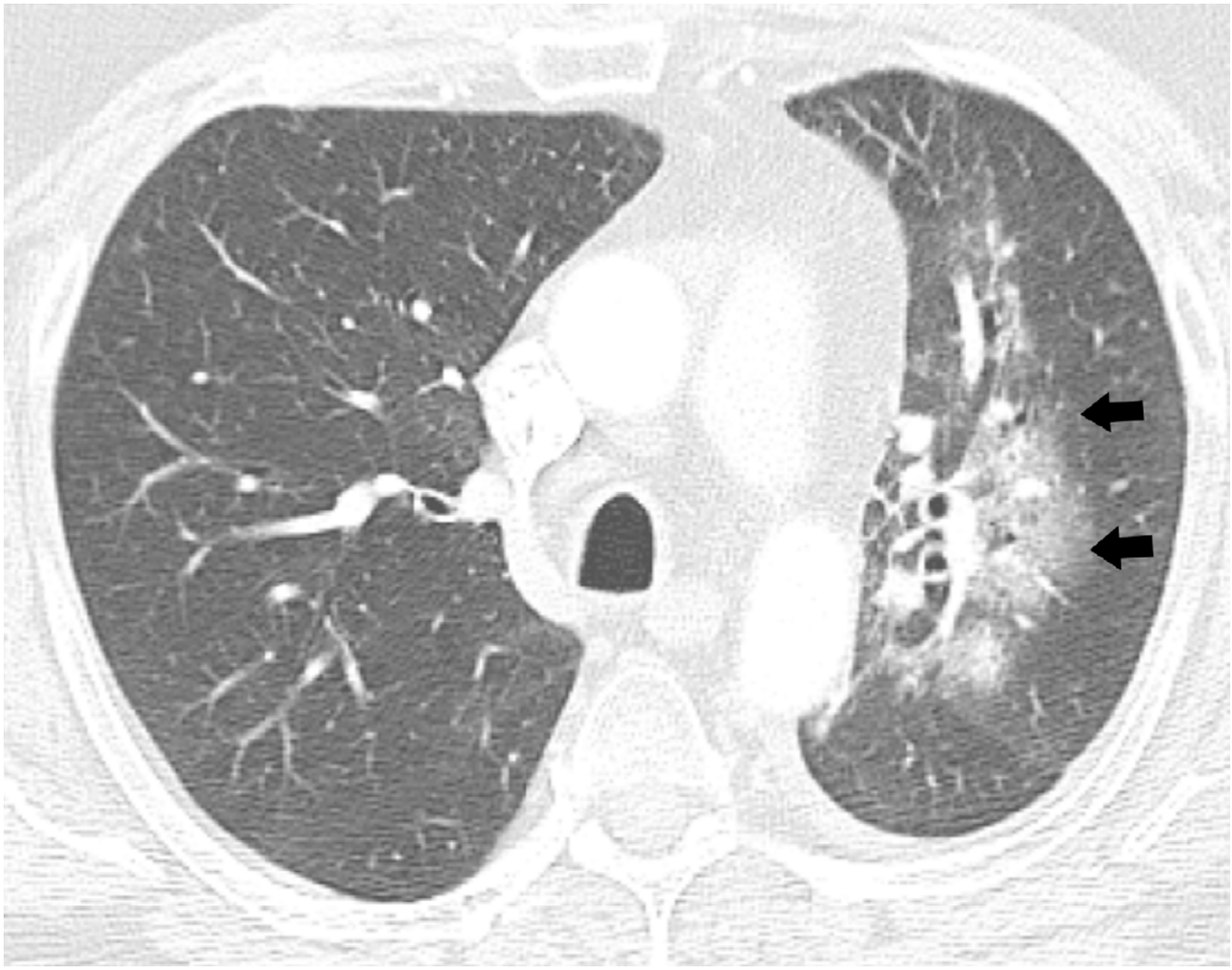

Fig 2. Fifty-two-year-old man with adenocarcinoma of the lung

(a) Axial CT image after administration of intravenous contrast medium and prior to treatment shows a left central lung lesion (arrow) surrounding lingular bronchus. (b) Axial CT image obtained 2 months after completion of radiotherapy shows ground-glass opacities (arrow) consistent with radiation lung injury.

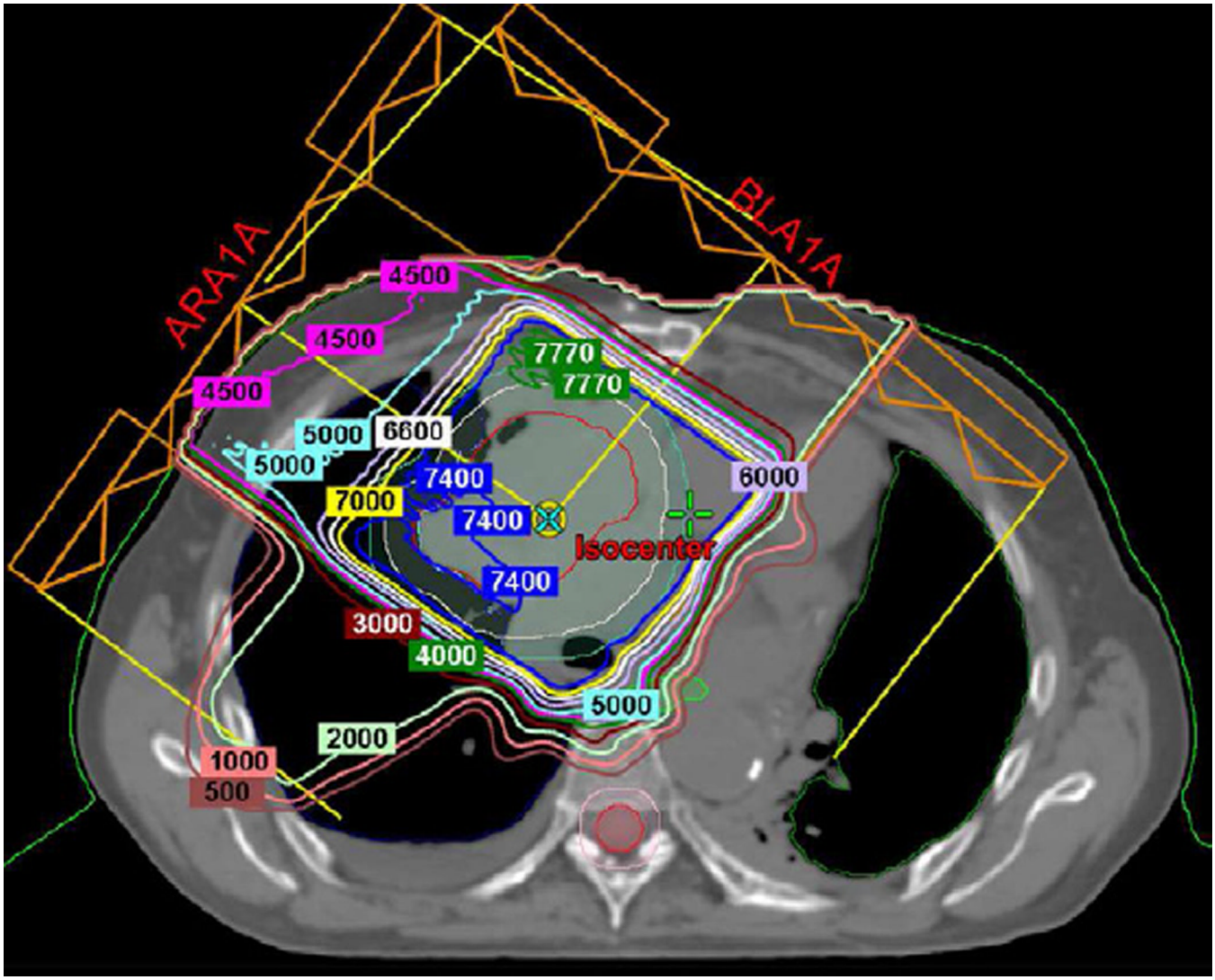

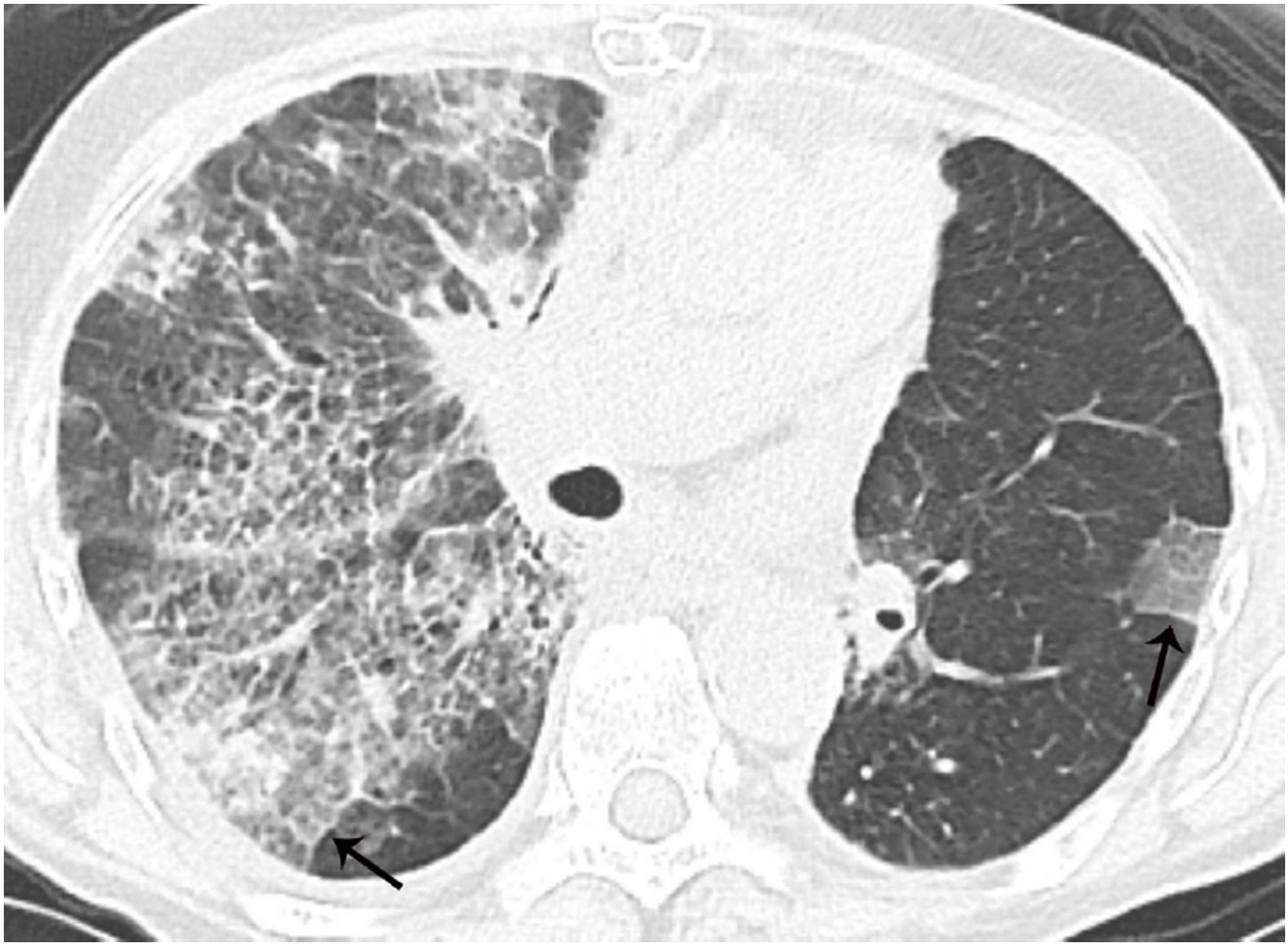

Fig. 3. Seventy-five-year-old woman with adenocarcinoma of the lung

(a) 3-D conformal proton beam radiation plan utilizing a right anterior oblique and a left anterior oblique beams and a total dose of 74 Co-60 Gy in 37 fractions.

(b) Axial CT image obtained 3 months after completion of radiotherapy shows ground-glass opacities with interlobular septal thickening in the right lung (arrow) consistent with a crazy-paving pattern. Note that there are focal left lung opacities outside of the radiation field consistent with post radiation changes.

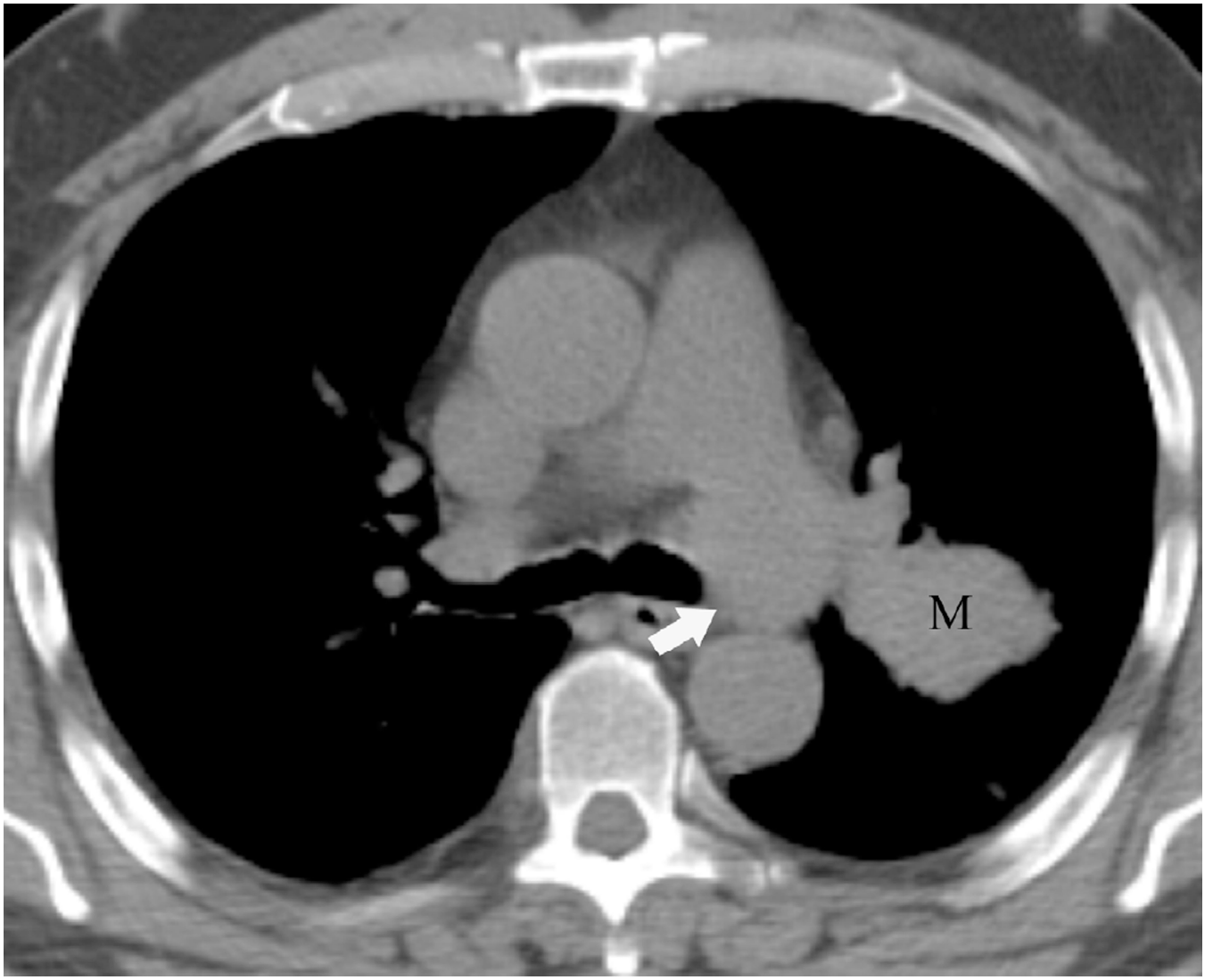

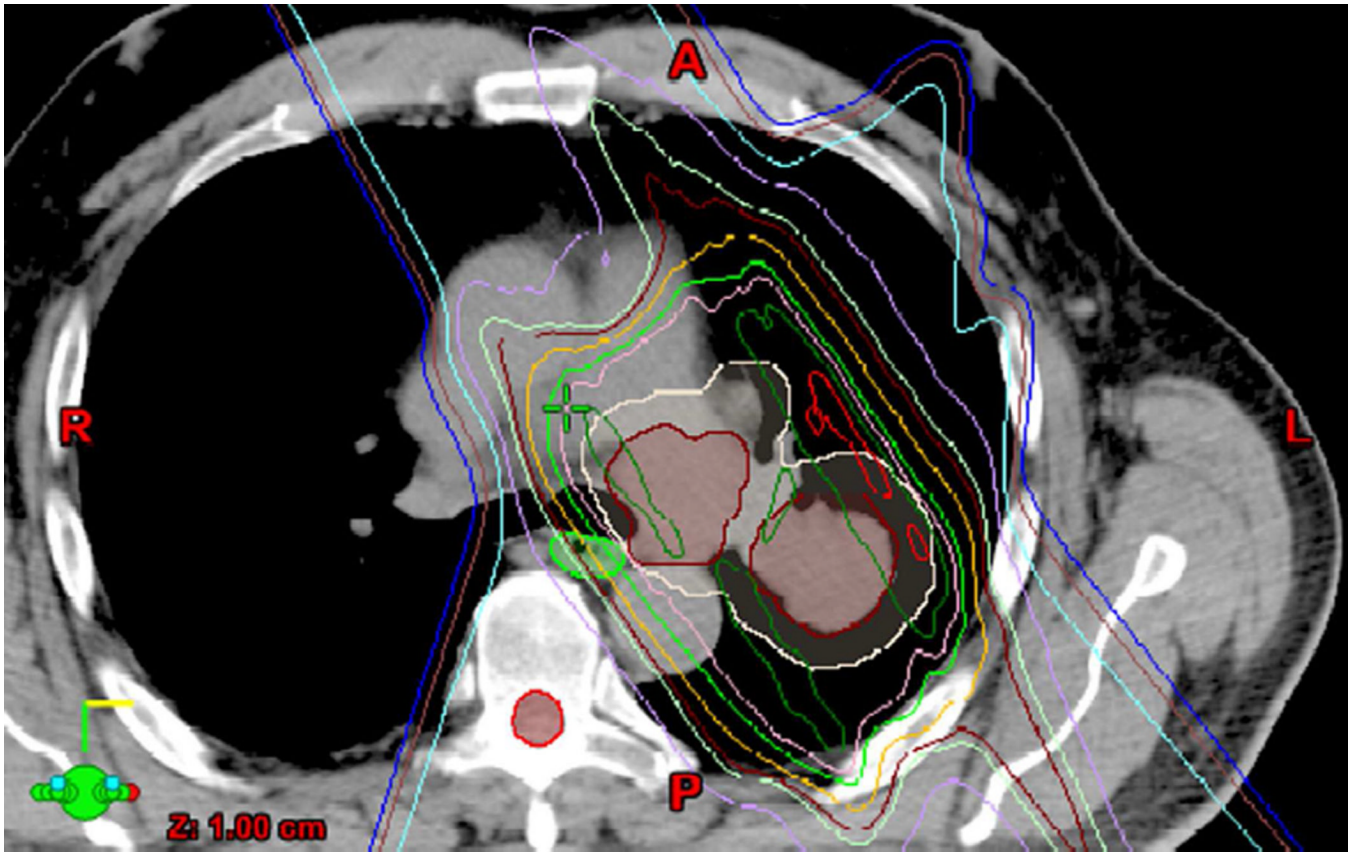

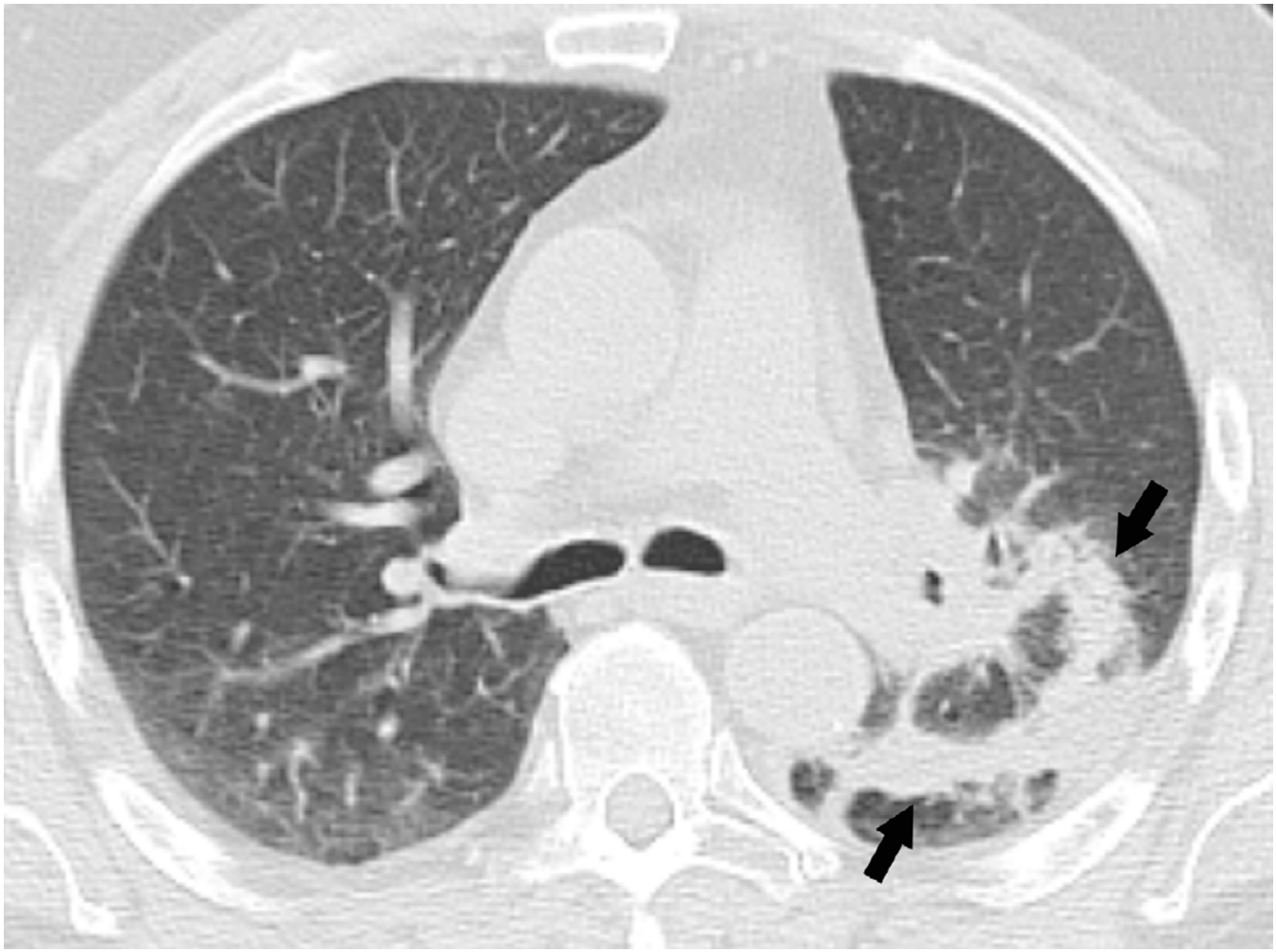

Fig. 4. Sixty-eight-year-old man with a left upper lobe NSCLC

(a) Axial CT image before administration of intravenous contrast medium and prior to radiotherapy treatment shows a large central left upper lobe mass (M) and left paratracheal nodal metastatic disease (arrow).

(b) 3D conformal proton beam radiation plan utilizing a right anterior oblique, left posterior oblique and right posterior oblique beams and a total dose of 74 Co-60 Gy in 37 fractions.

(c) Axial CT image obtained 4 months after completion of radiotherapy demonstrating a central ground-glass opacity with a surrounding halo of consolidation (arrows) consistent with a reversed halo sign.

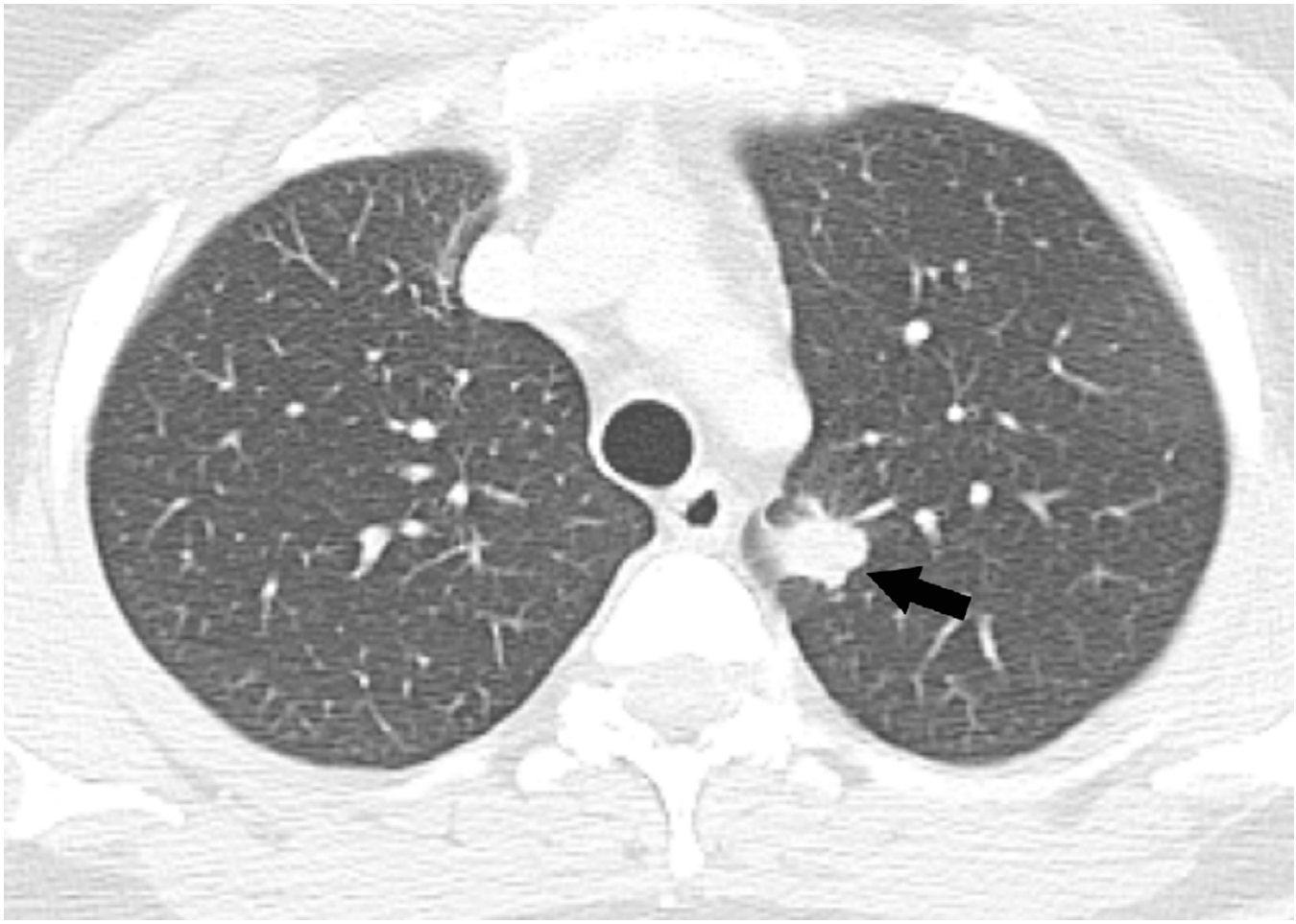

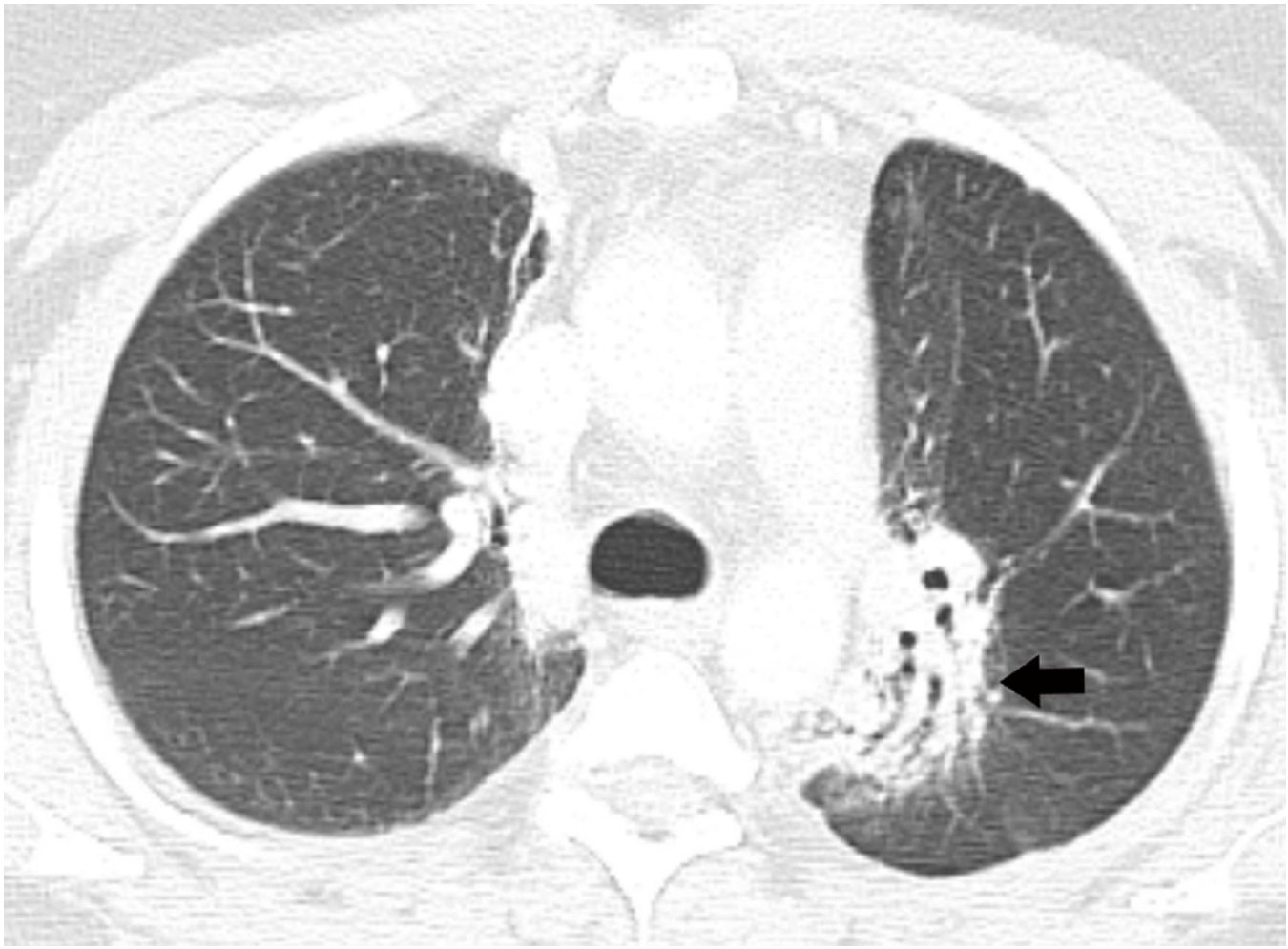

Fig 5. Thirty-six-year-old woman with a left upper lobe NSCLC

(a) Axial CT image prior to treatment show a spiculate nodule in the left upper lobe (arrow). (b) Axial CT image obtained 3 years after completion of radiotherapy shows lung opacities with traction bronchiectasis (arrow) consistent with radiation fibrosis.

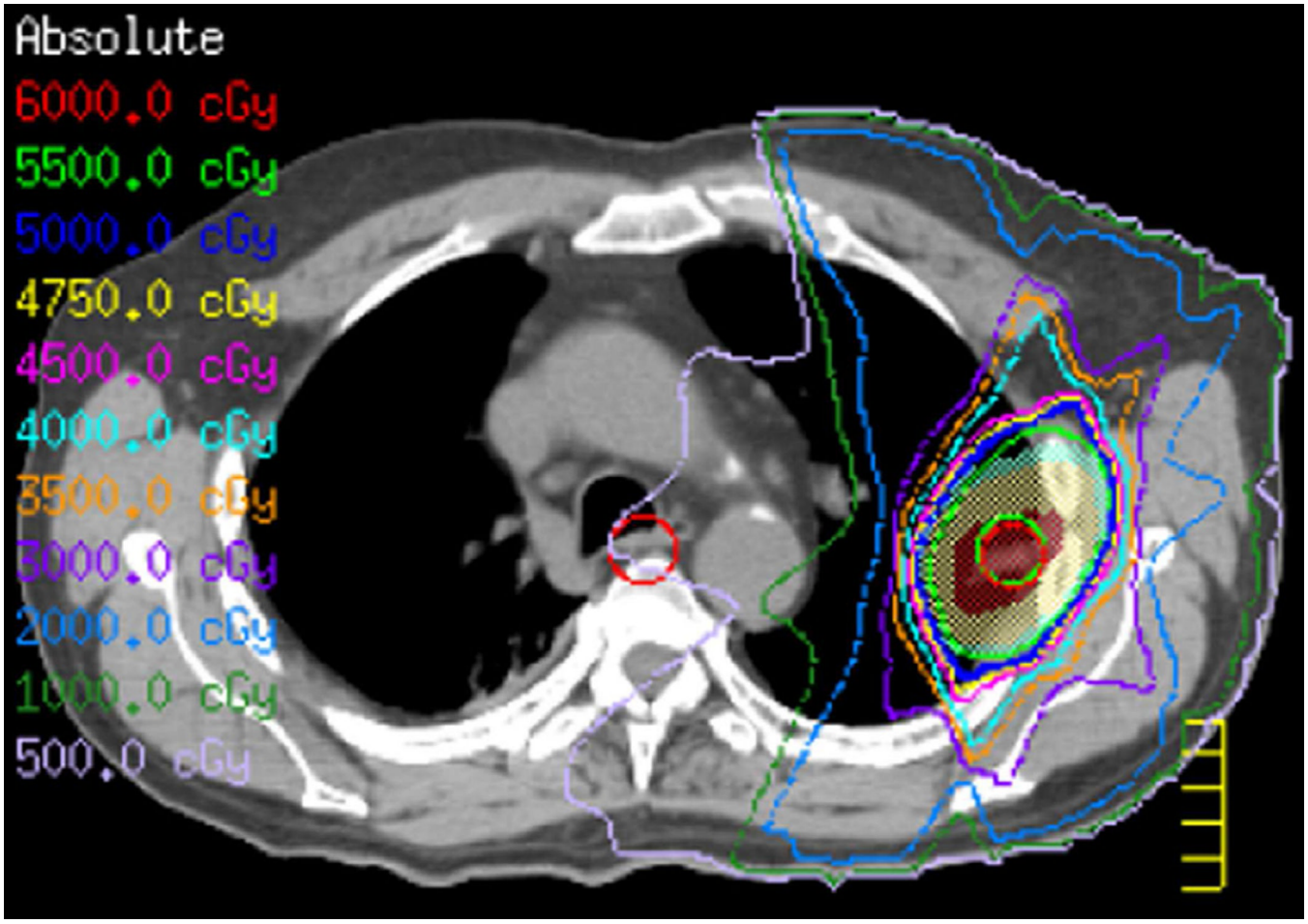

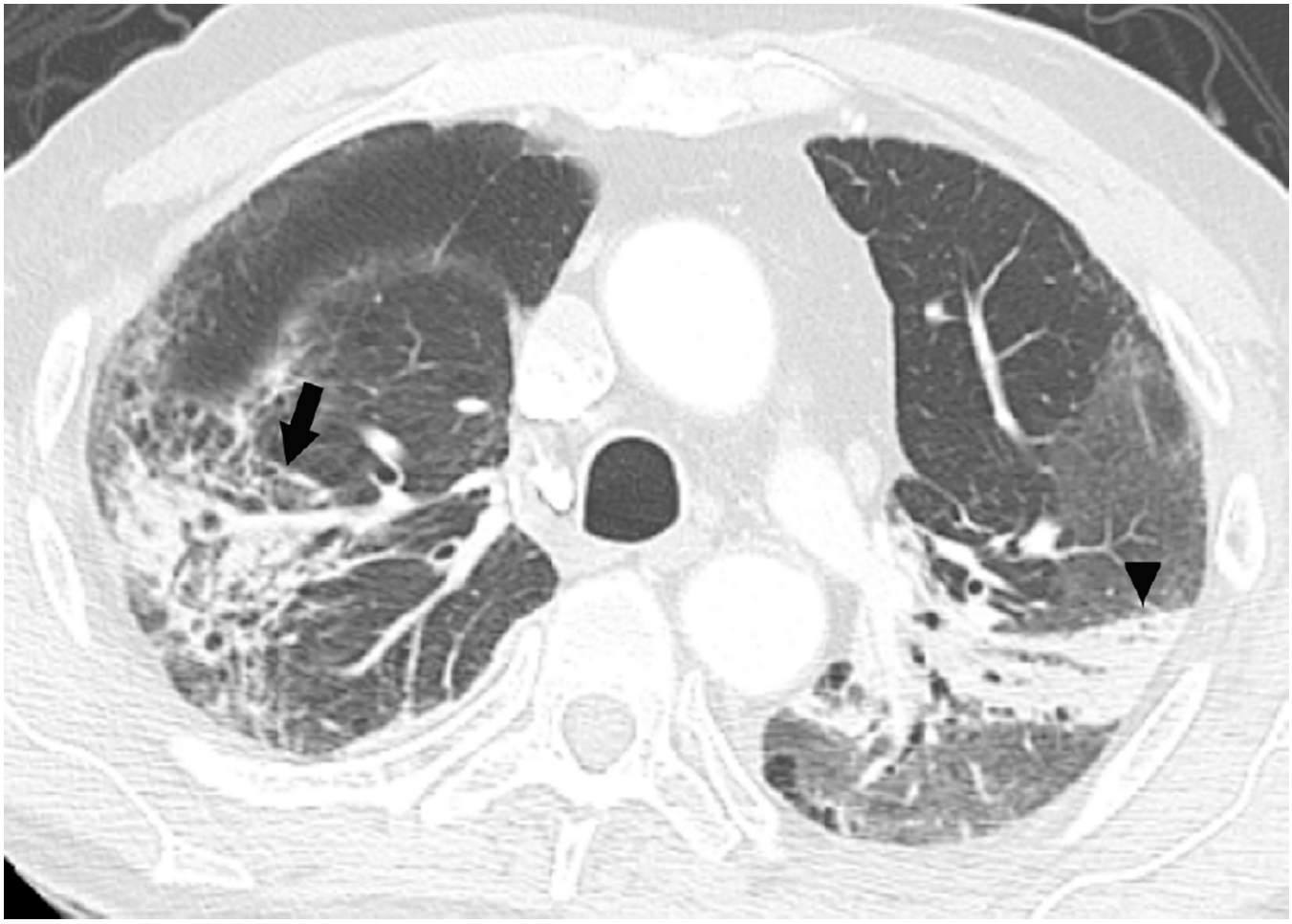

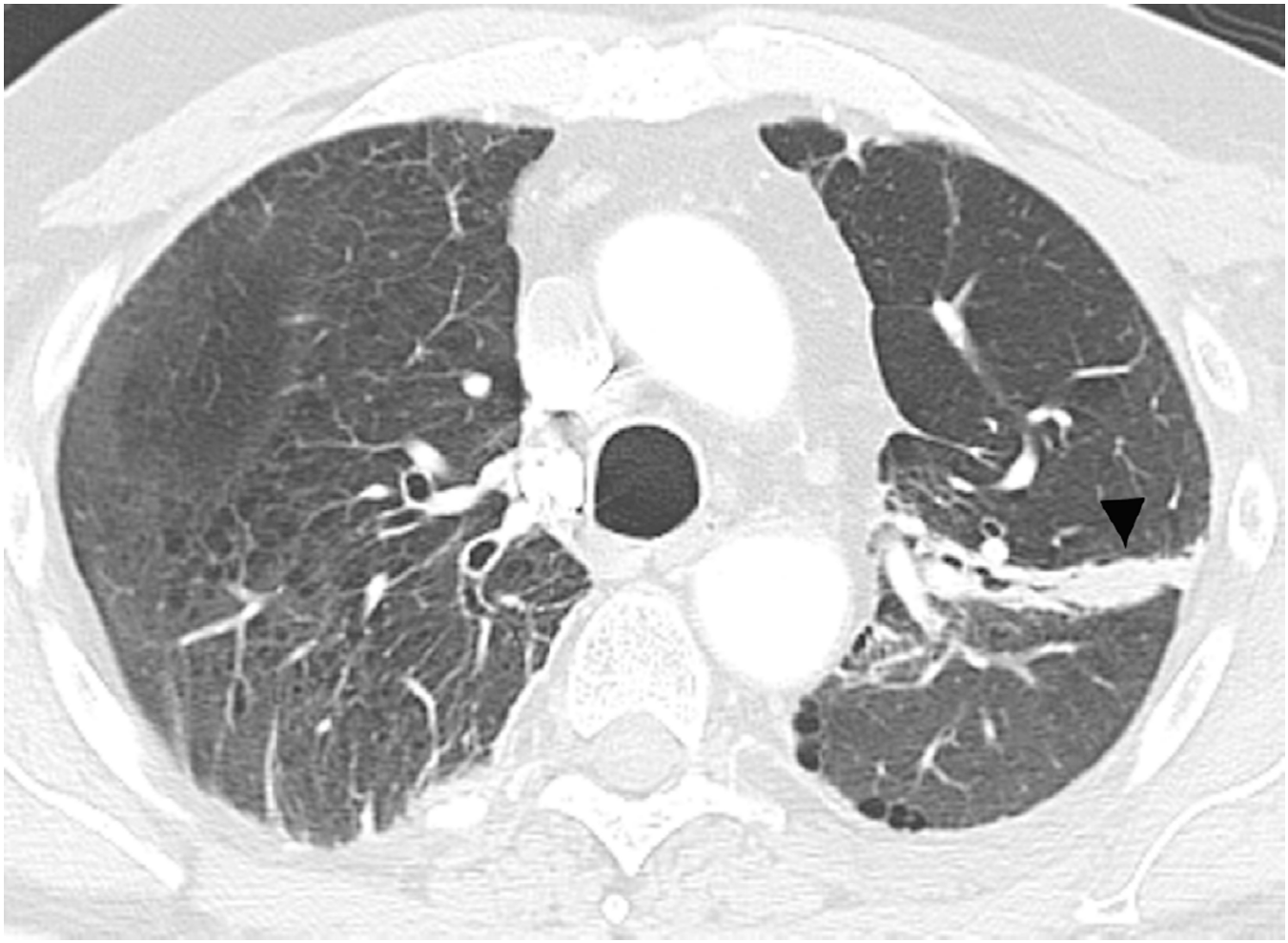

Fig. 6. Sixty-eight-year-old man with a left upper lobe NSCLC treated with stereotactic body radiotherapy

(a) Treatment planning field in SBRT. A total dose of 50 Gy in four fractions was delivered.
(b) Axial CT image 6 months after completion of therapy shows focal lung opacities in the left lung included in the irradiated field (arrowhead) and consistent with radiation lung damage. In the right lung there are new opacities far from the radiation planning area (arrow).
(c) Axial CT image obtained 8 months after completion of RT demonstrate persistence of RILD (arrowhead) with resolution of right upper lobe pneumonia.

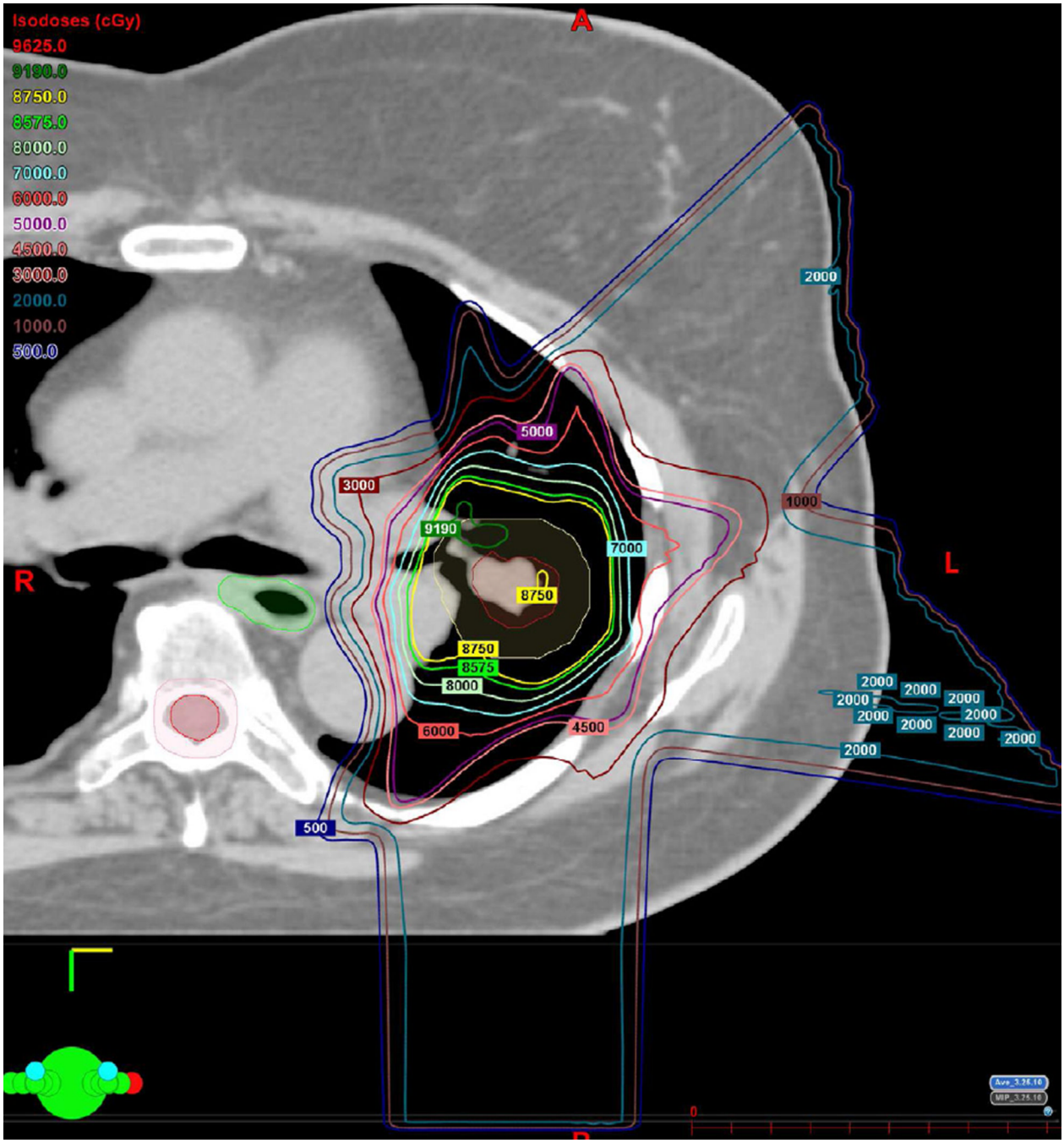

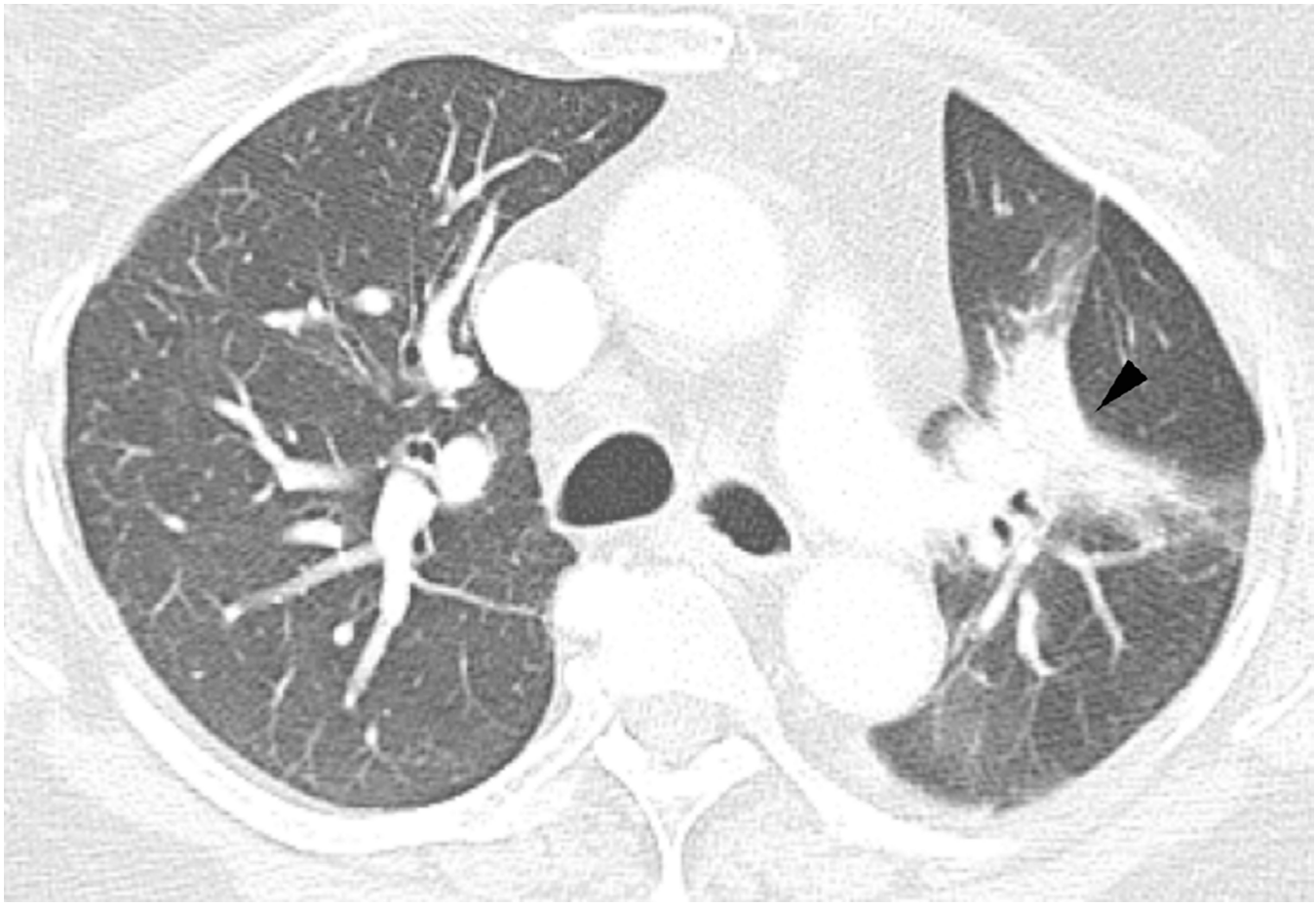

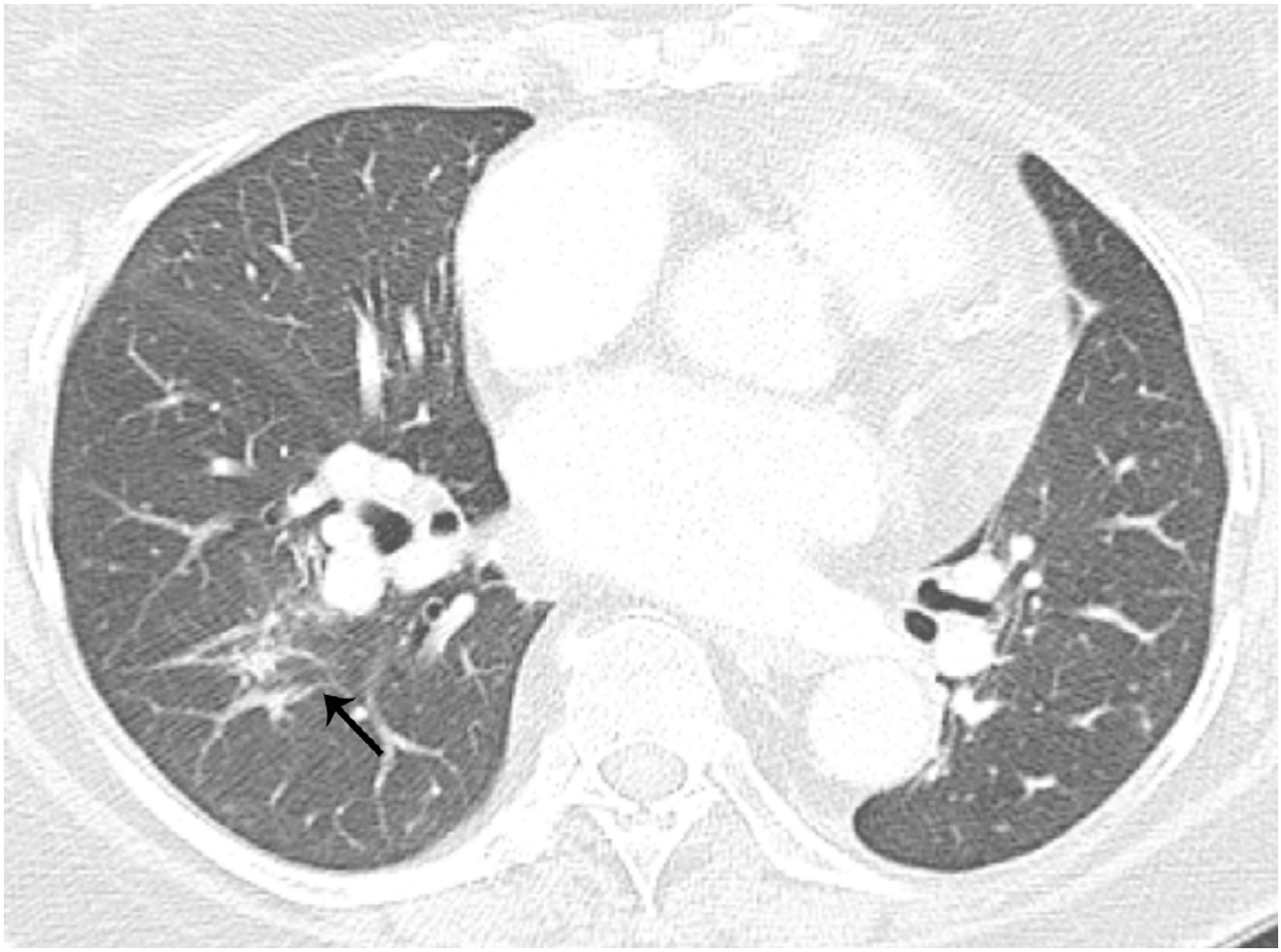

Fig. 7. Sixty-six-year-old woman with left upper lobe lung cancer treated with definitive proton radiation therapy

Six months after treatment completion patient had a primary complaint of cough and shortness of breath.

(a) Treatment planning field included three beams and a total dose of 87.5 Co-60 Gy. Proton therapy was chosen due to the fact that the tumour is located close to lobar bronchus and proton radiation therapy would be the optimal way of treating this tumour to reduce toxicity and possible bronchial stenosis.

(b) Axial CT image obtained 6 months after completion of therapy demonstrates left lung opacities included in the irradiated filed (*) consistent with radiation lung injury. There is additional development of focal right upper lobe opacity (arrow) outside of the treatment planning field.

(c) Axial CT images obtained 8 months after completion of therapy demonstrates persistent post-radiation lung injury in the left upper lobe (arrowhead) with resolution of the right upper lobe consolidative opacity.

(d) Axial CT image obtained 8 months after completion of therapy at a lower anatomic level than (c), detected migratory patchy lung opacities (thin arrow). Right upper lobe opacities detected on Fig. 10b have resolved in the interval. A clinical diagnosis of organizing pneumonia was made and treatment with steroid was indicated. Patient demonstrated clinical improvement and prednisone was gradually tapered and totally discontinued. After 4 months chest CT (not shown) demonstrated completed resolution of radiological findings.

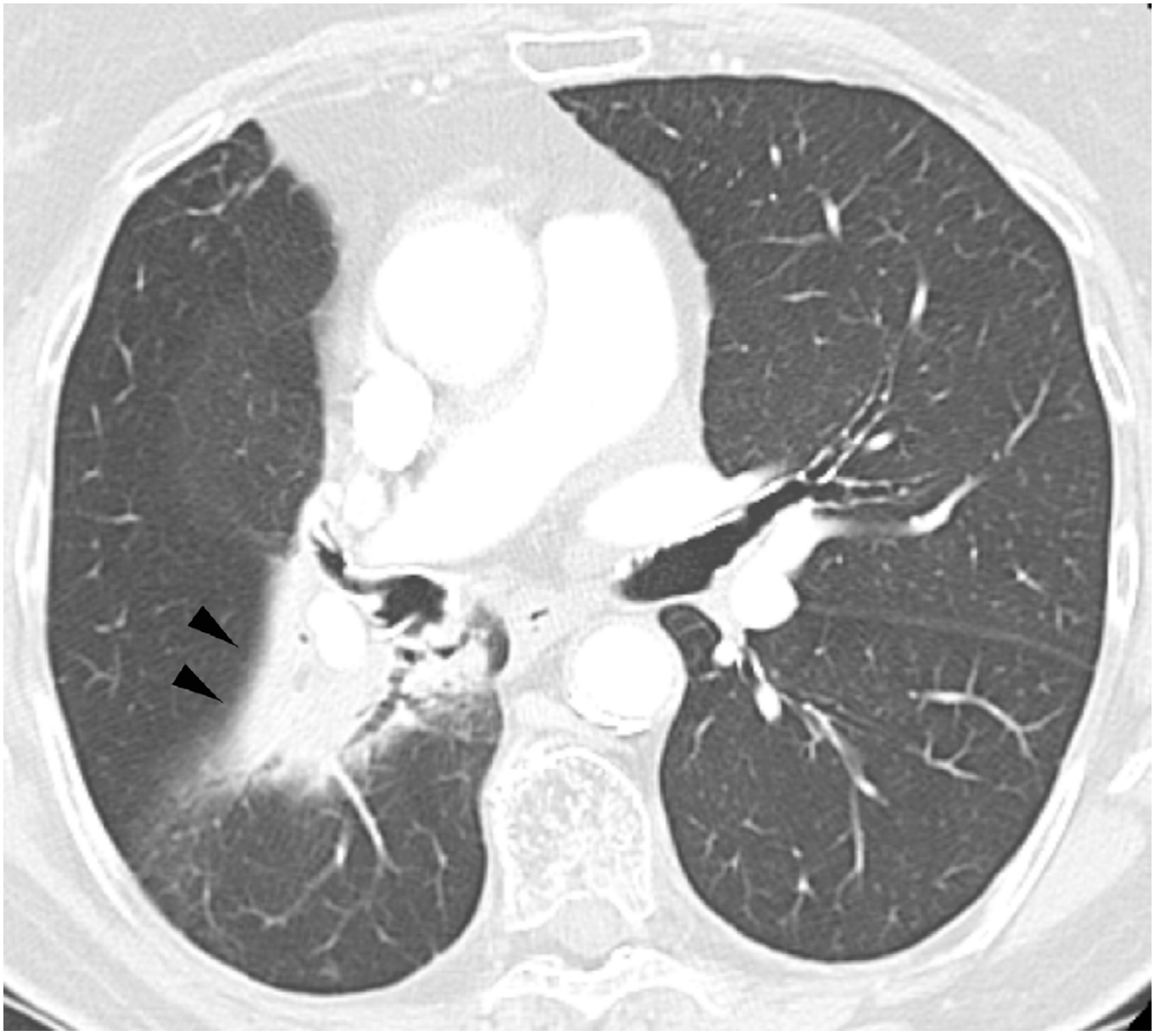

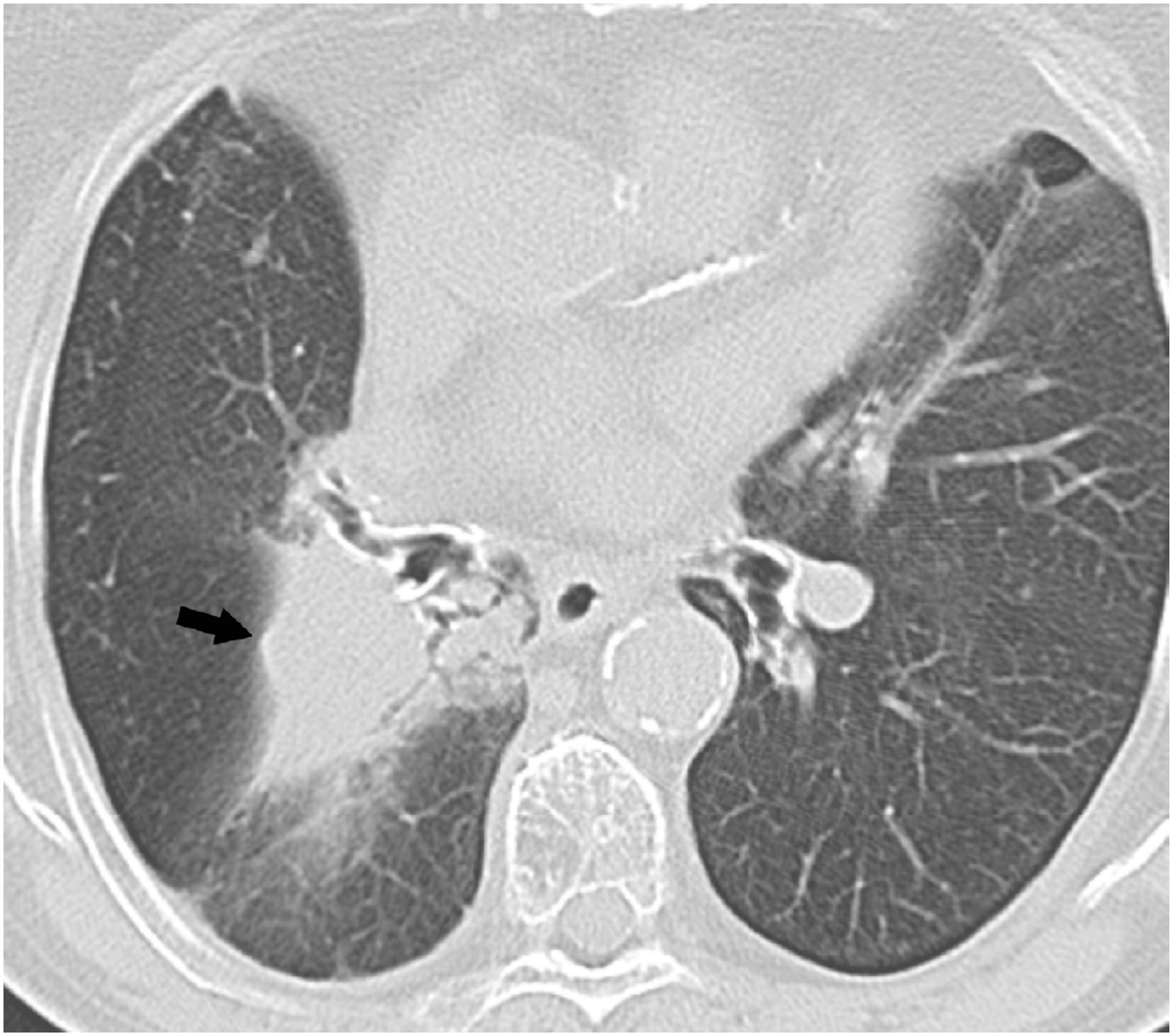

Fig. 8. An 87-year-old woman with a diagnosis of stage II NSCLC treated with definitive radiotherapy

(a) Axial CT image obtained 2 years after treatment ending demonstrate focal lung opacities with traction bronchiectasis and architectural distortion consistent with radiation fibrosis. Note sharp lateral border (arrowheads) consistent with post radiation changes.
(b) Axial CT image obtained 4 years after treatment completion demonstrates lobulation of the lateral border suspicious for recurrent tumour (arrow).
(c) PET-CT demonstrated FDG avidity in the suspected lesion. A lung biopsy confirmed the diagnosis of recurrent tumour.

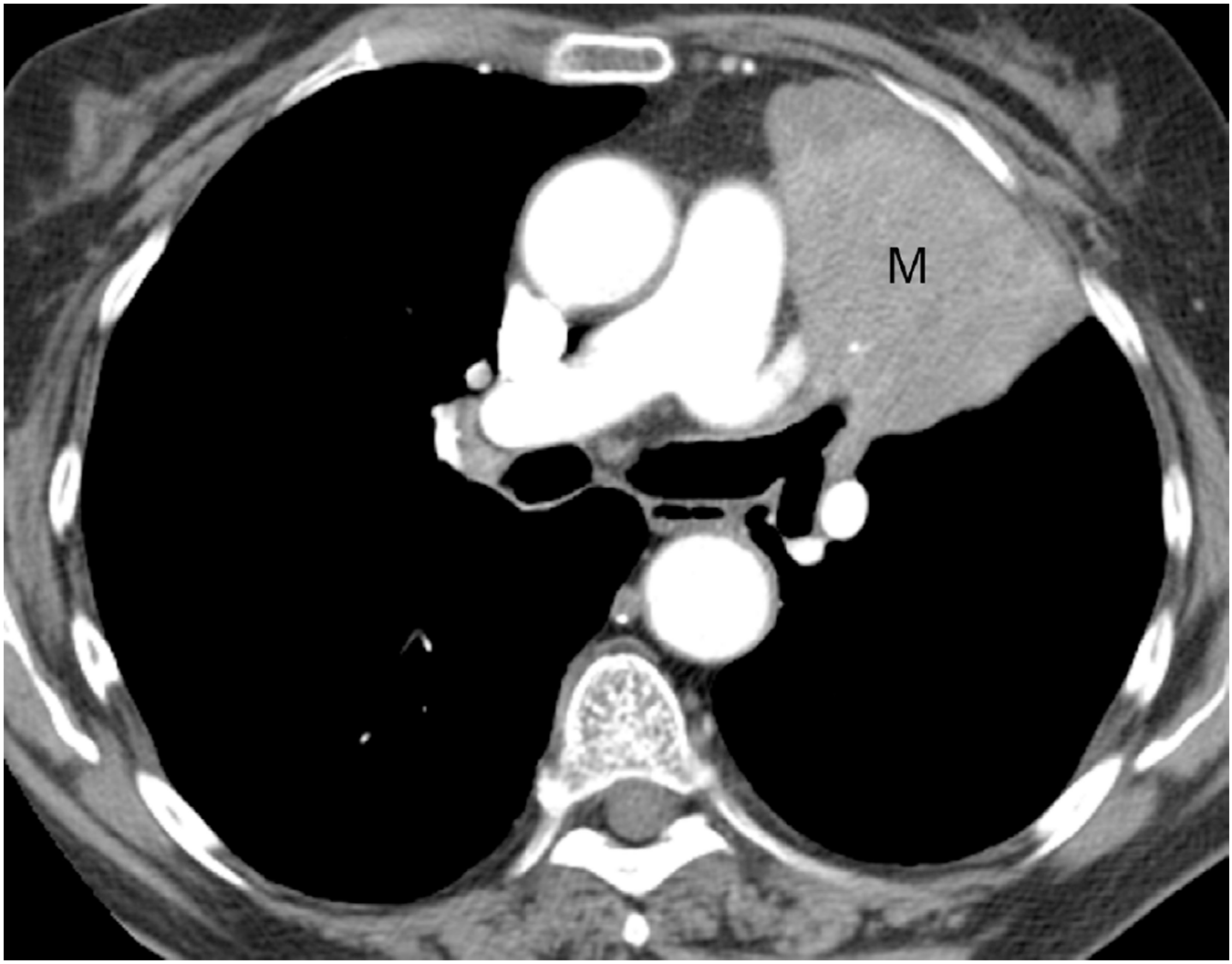

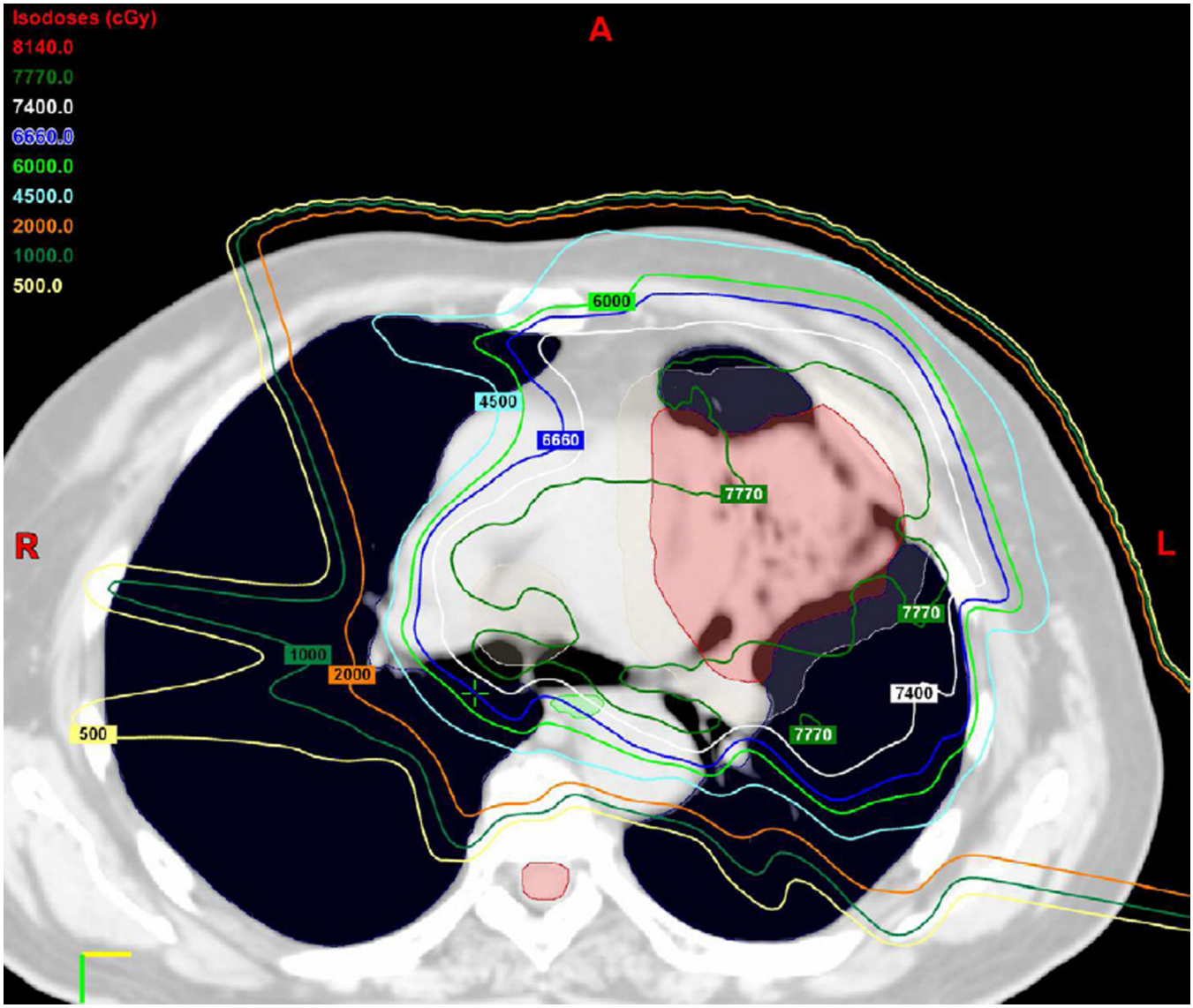

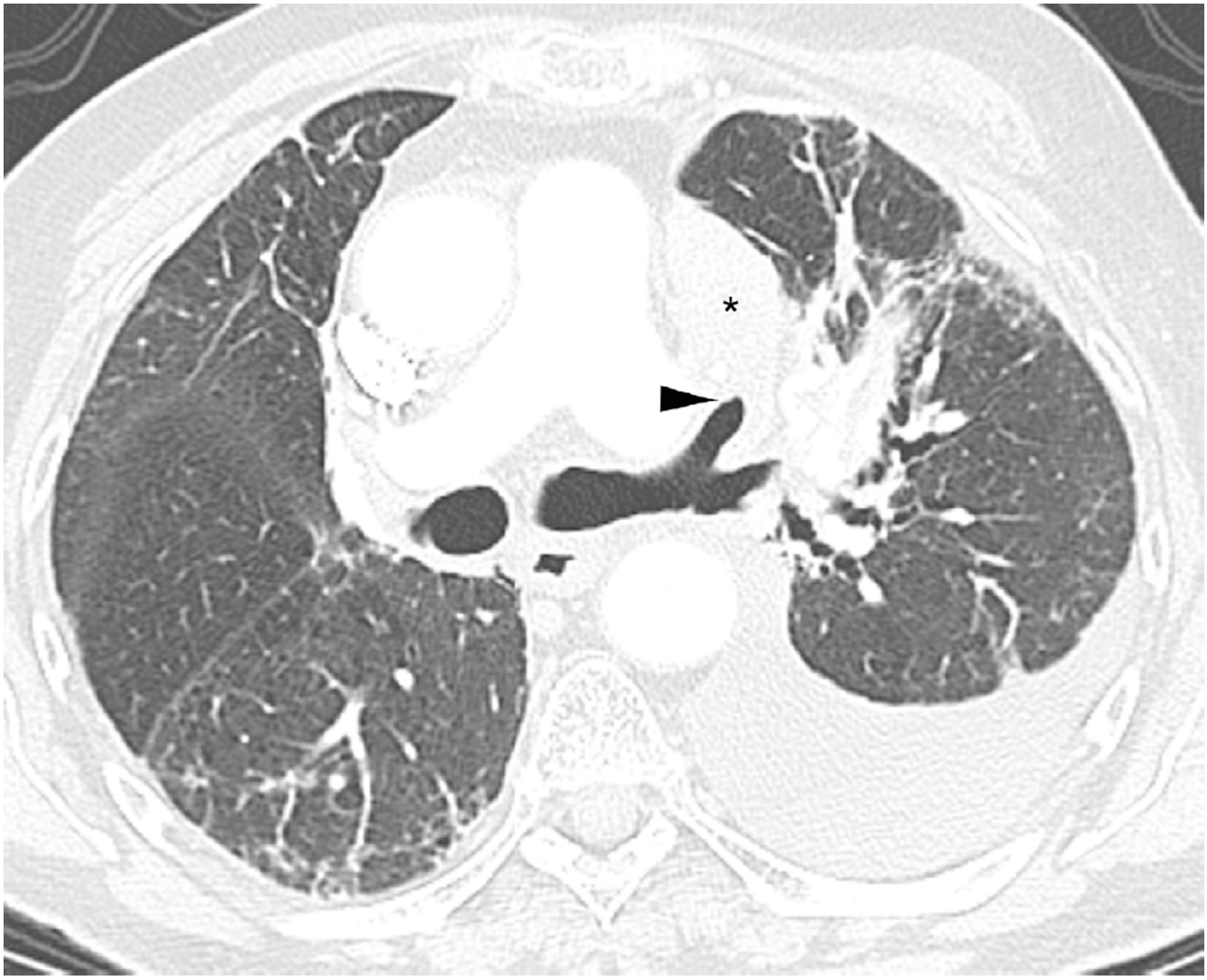

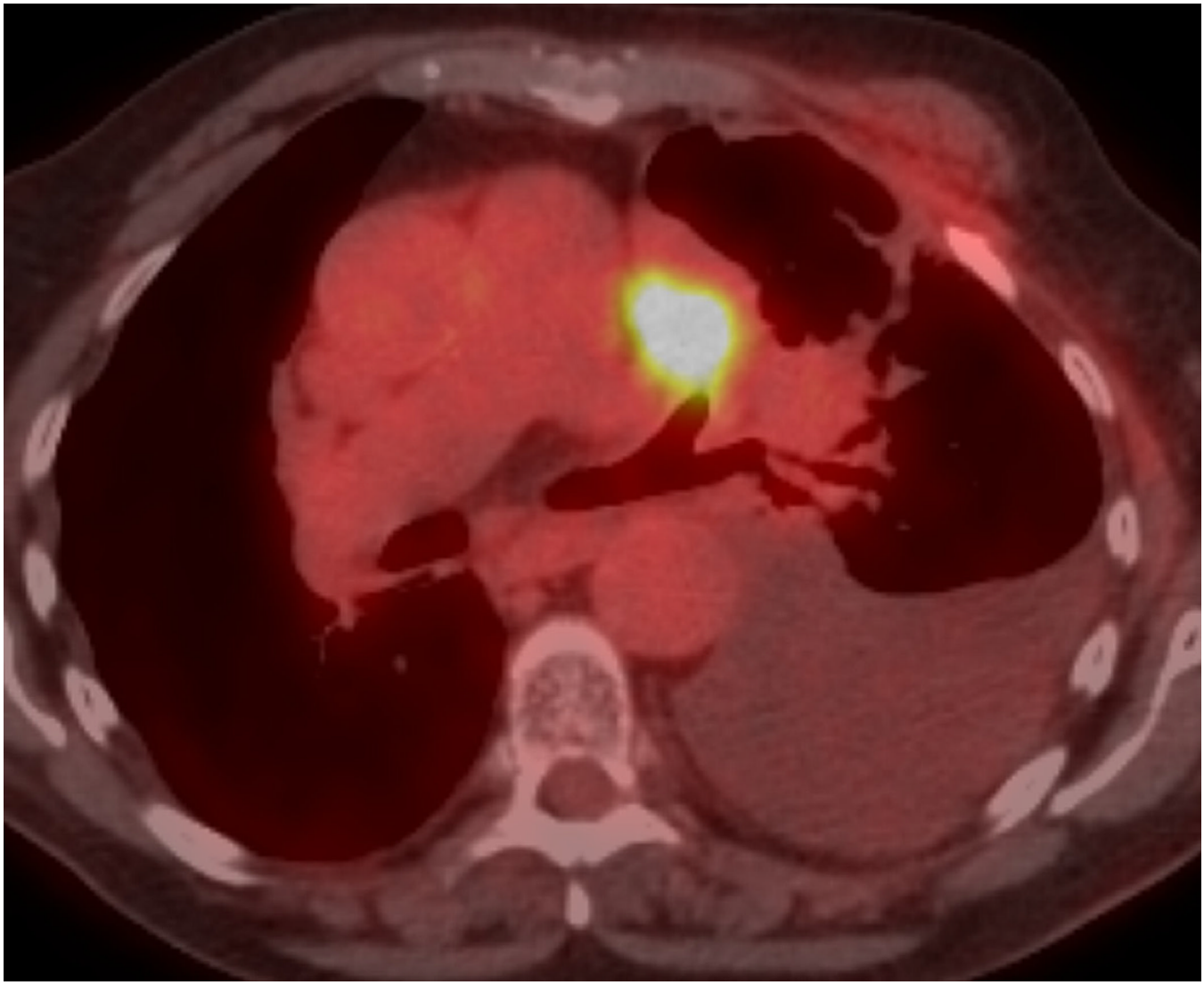

Fig. 9. A 77-year-old woman with left upper lobe squamous cell carcinoma of the lung

(a) Axial CT image after administration of intravenous contrast medium shows a large left upper lobe mass (M) extending to the hilar region and obstructing the left upper lobe bronchus.

(b) Treatment planning field include the left upper lobe and mediastinum treated with proton therapy with a total dose of 74 Co-60 Gy.

(c) Axial CT image 12 months after completion of therapy demonstrated a new soft-tissue nodular opacity (*) anterior to the left upper lobe bronchus (arrowhead). Note is also made of a new left pleural effusion developed after 6 months after completion of radiation therapy.

(d) PET-CT shows a nodular FDG uptake included in the irradiated area. A recurrent tumour was diagnosed at biopsy.

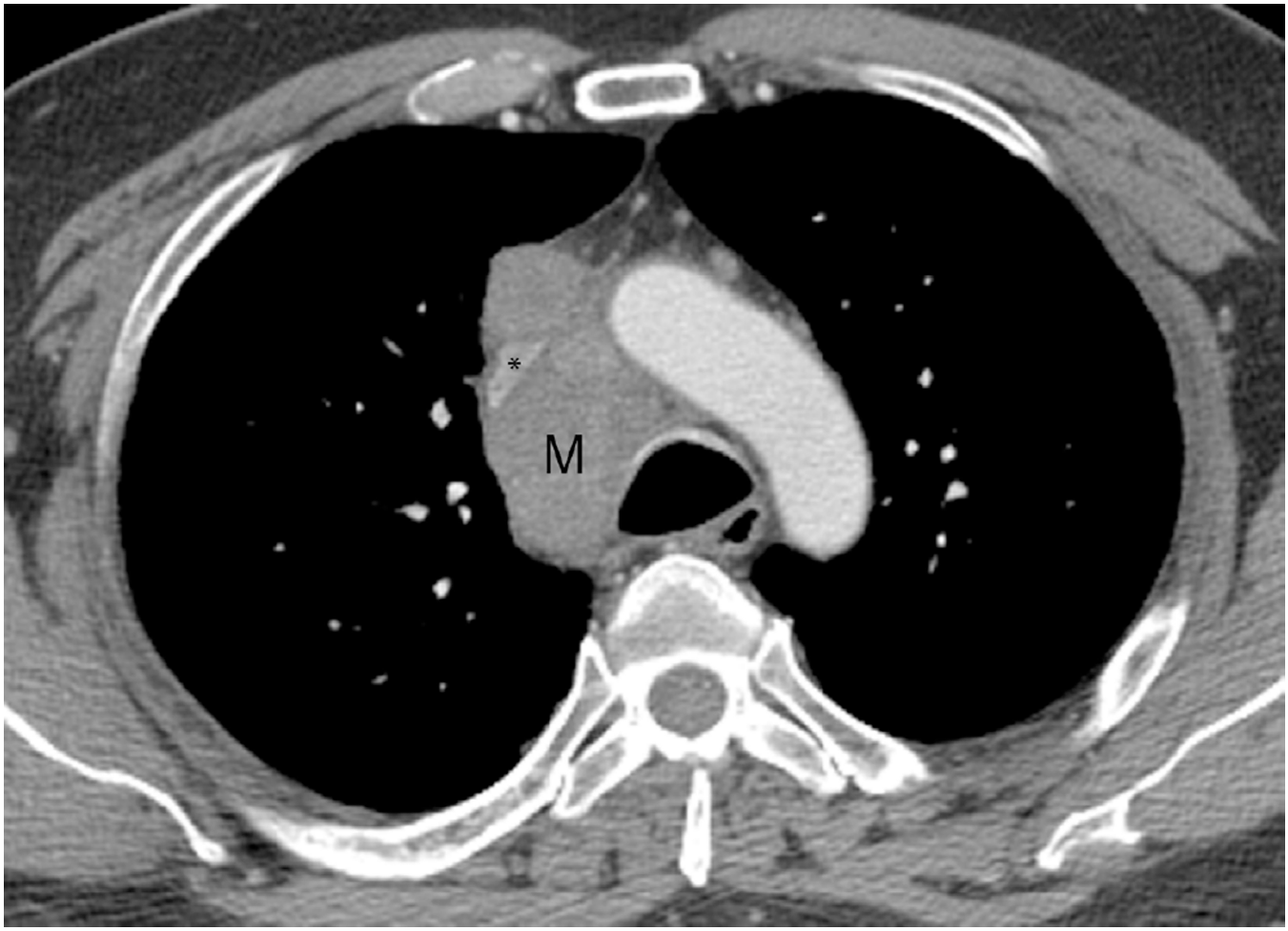

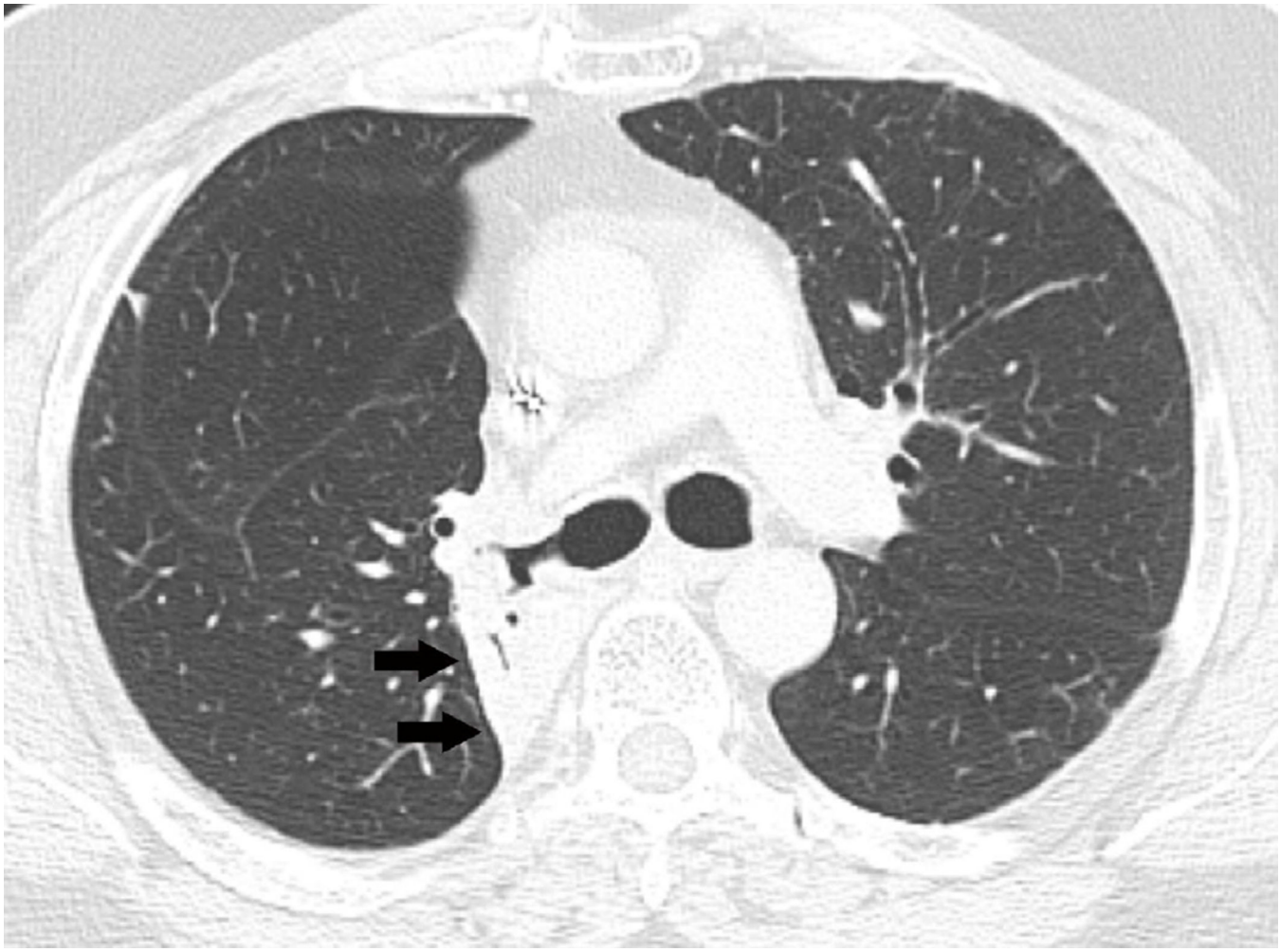

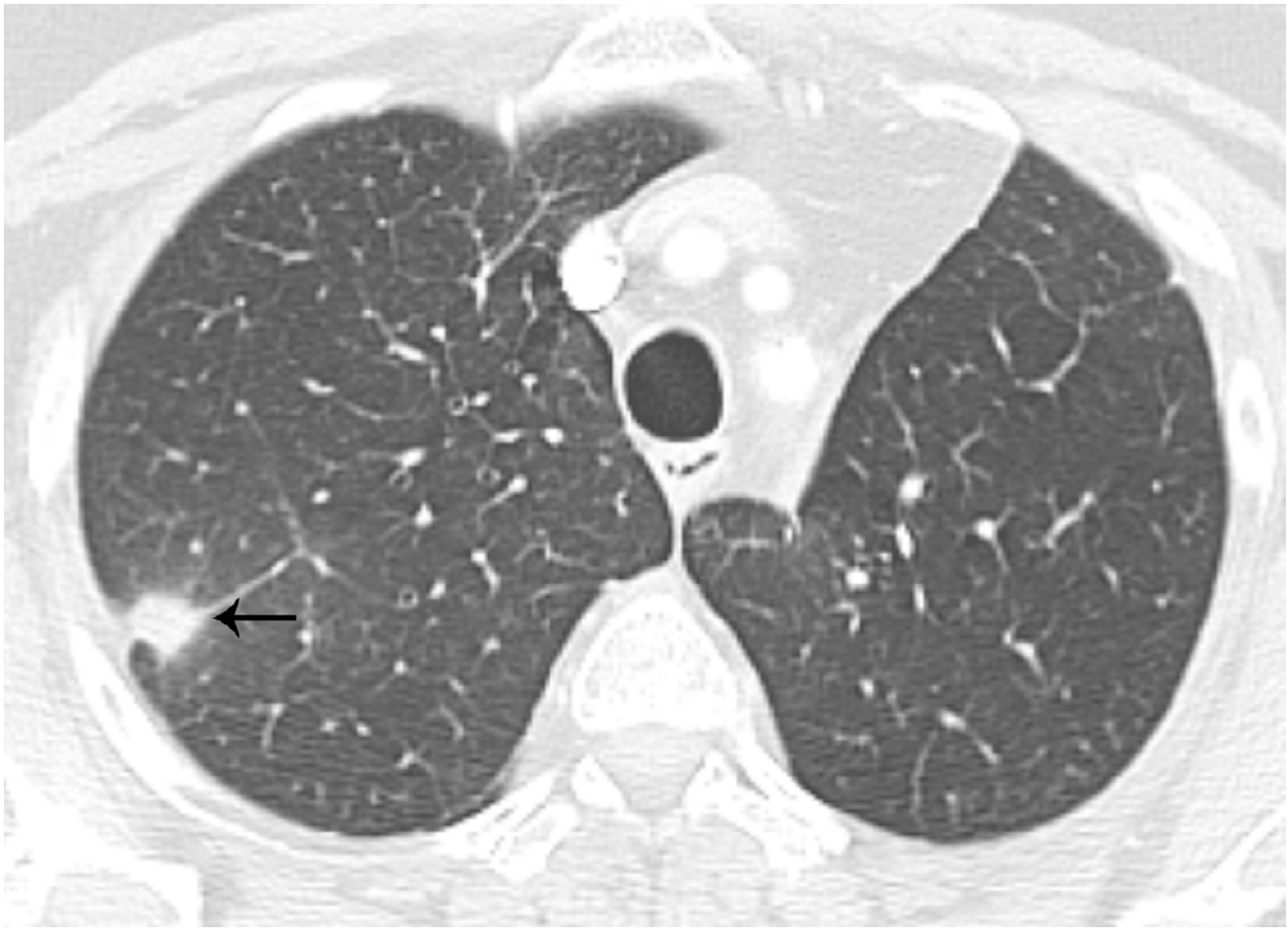

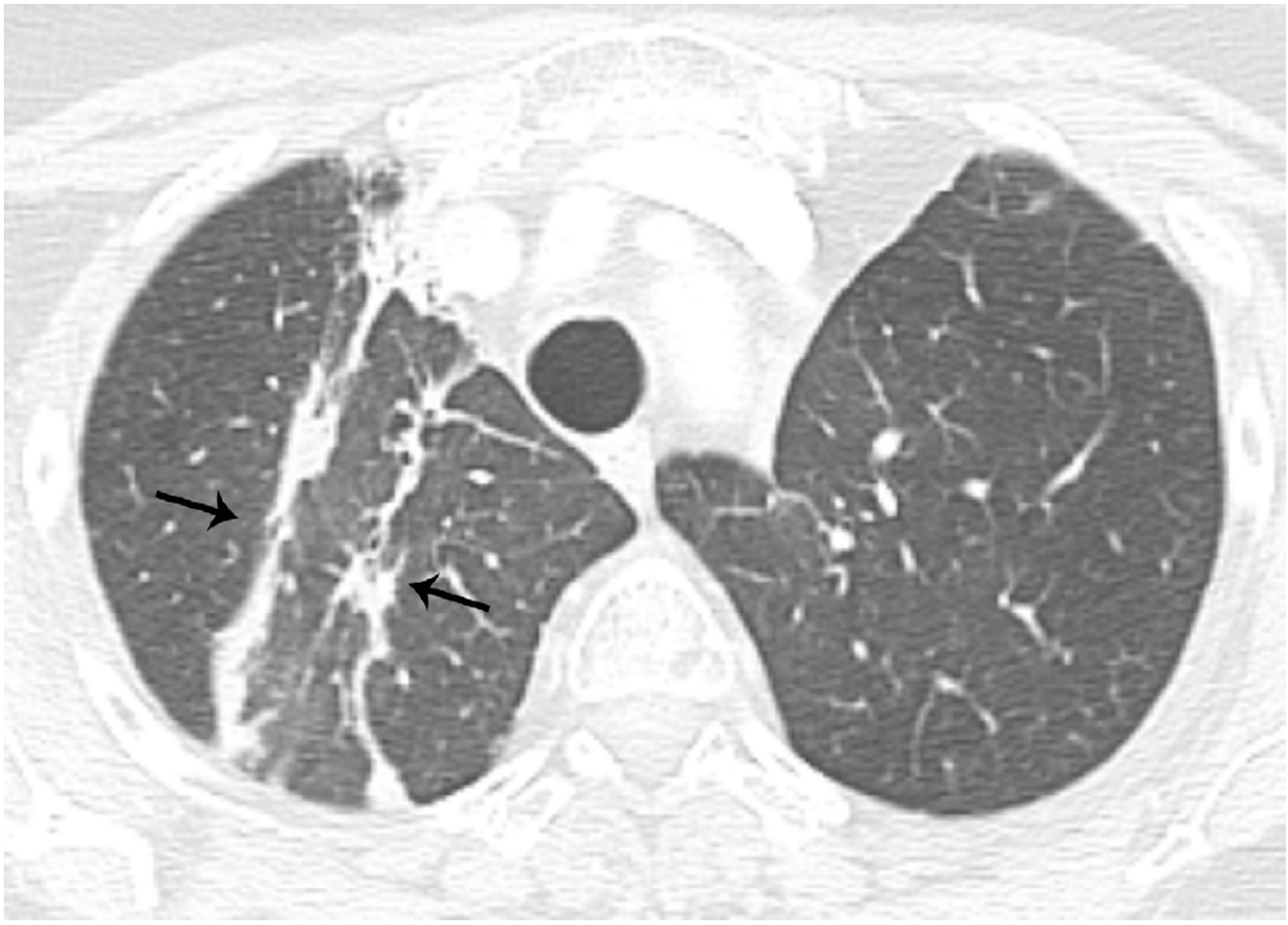

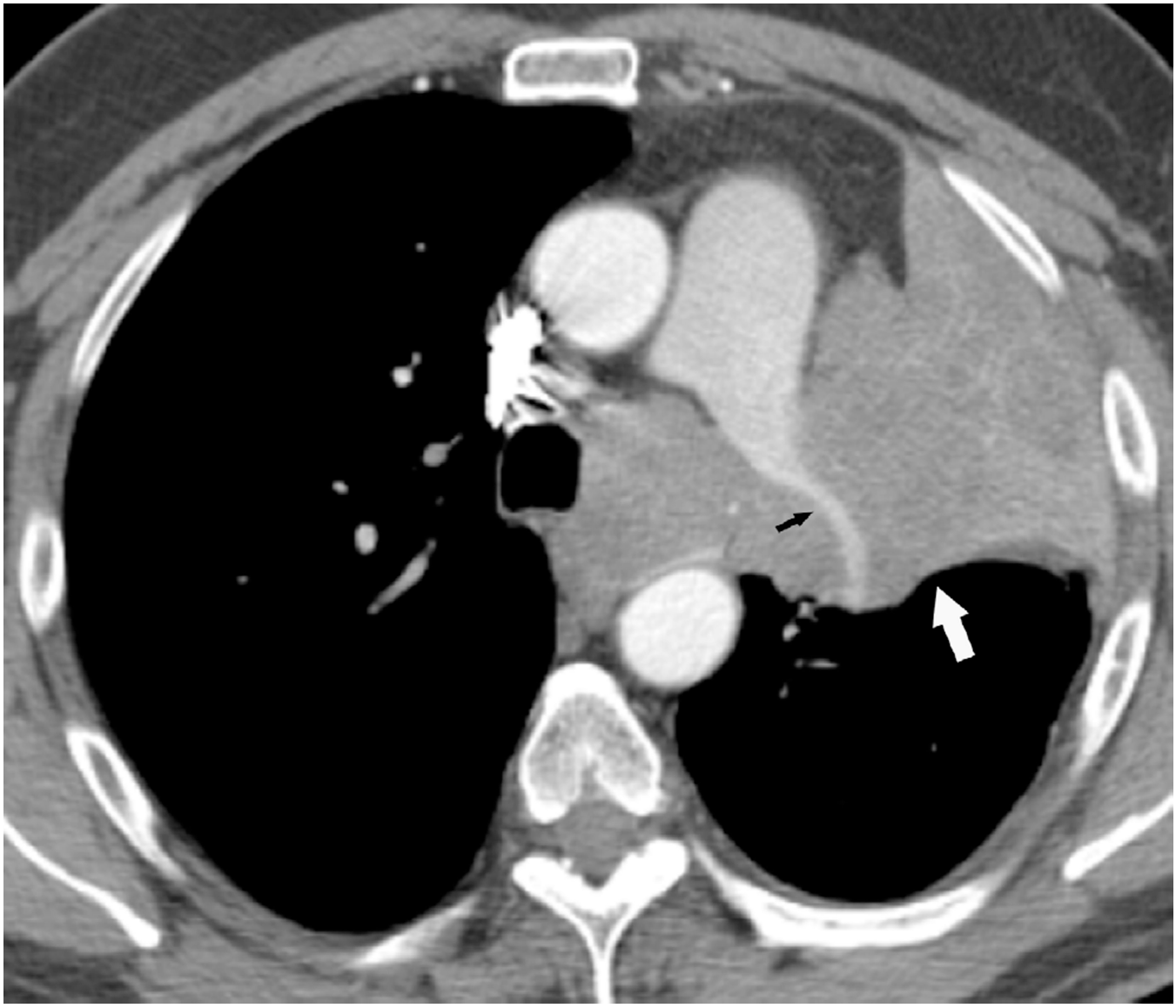

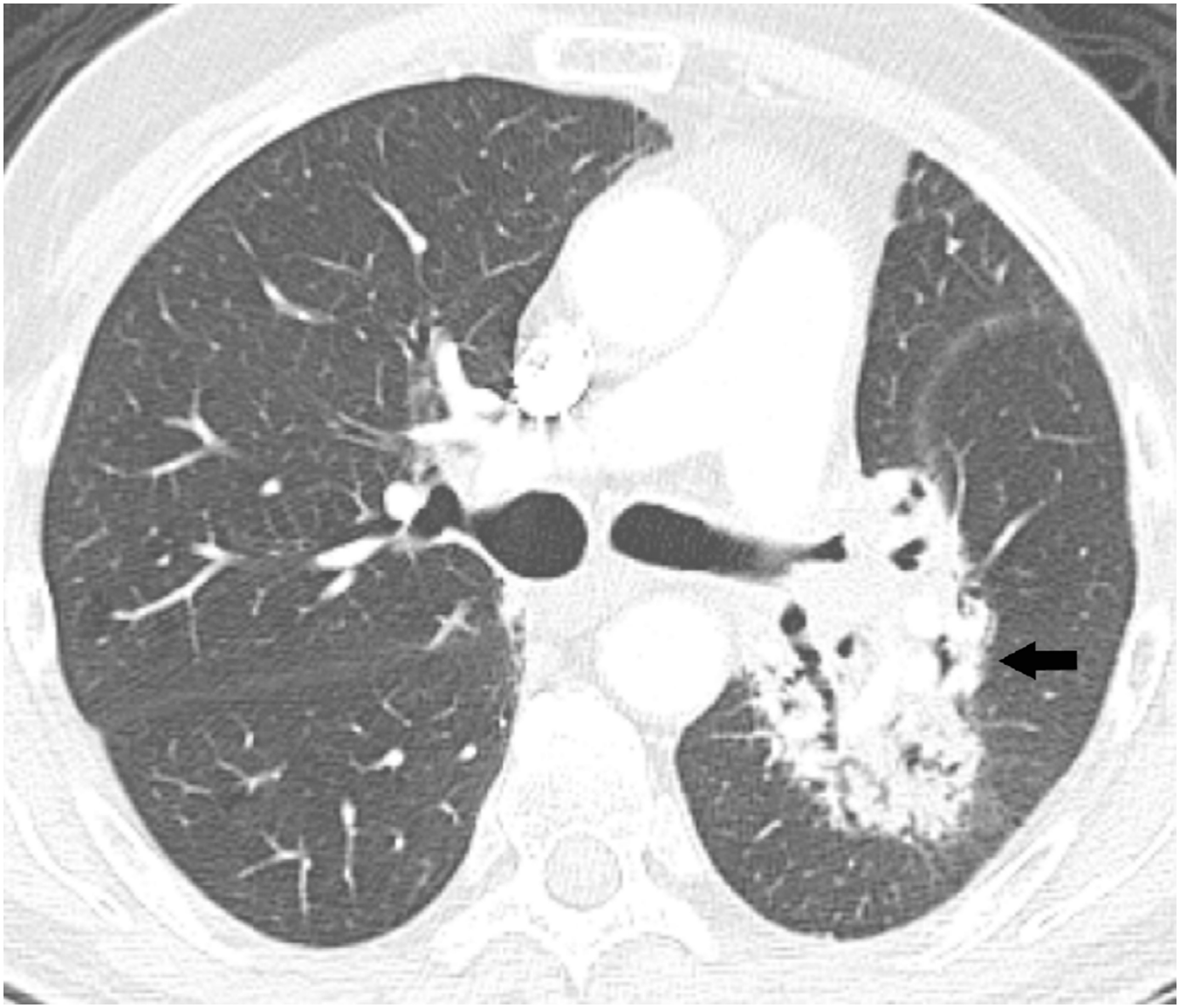

Fig. 10. Different radiological appearance after 3D CRT in patients with history of lung cancer and submitted to radiotherapy

(a–b) A 62-year-old man with a diagnosis of adenocarcinoma in the right upper lobe with bulky mediastinal adenopathy. Axial CT image with intravenous contrast medium (a) obtained prior to treatment showing a large right paratracheal mass (M) compressing the superior vena cava (SVC) (*) consistent with nodal metastatic disease. Axial CT image 2 years after completion of radiation therapy (b) shows well-defined area of consolidation (arrows), volume loss, and traction bronchiectasis typical of modified conventional pattern of radiation fibrosis. (c–d) A 60-year-old woman with metastatic NSCLC. Axial CT image obtained prior to treatment shows a right upper lobe nodule (arrow) abutting the pleural surface (c). Axial CT image 8 months post-radiotherapy (d) shows linear lung opacities in the right upper lobe (thin arrows) that resembles scarring tissue and are consistent with a scar-like pattern. (e–f) A 57-year-old man with NSCLC treated with 3D CRT. Axial CT image with intravenous contrast medium (e) obtained prior to treatment shows a large left upper lobe mass (white arrow) surrounding and narrowing the left main pulmonary artery (black arrow). Note tumour involvement in the left paratracheal region. Axial CT image

obtained 18 months after completion of therapy (f) demonstrates lung opacities, patent bronchi, and bronchiectasis with mass-like appearance consistent with radiation fibrosis (arrow).

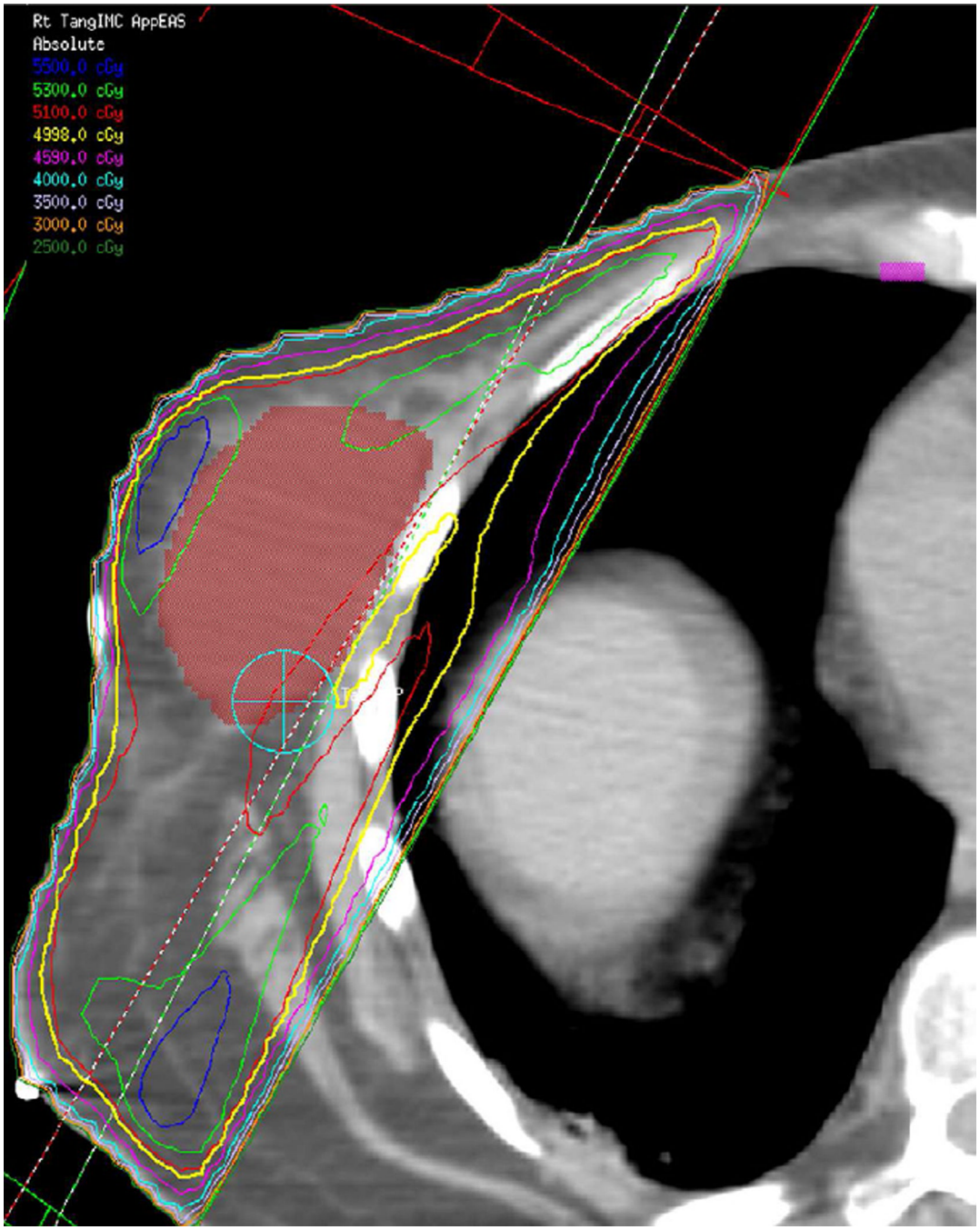

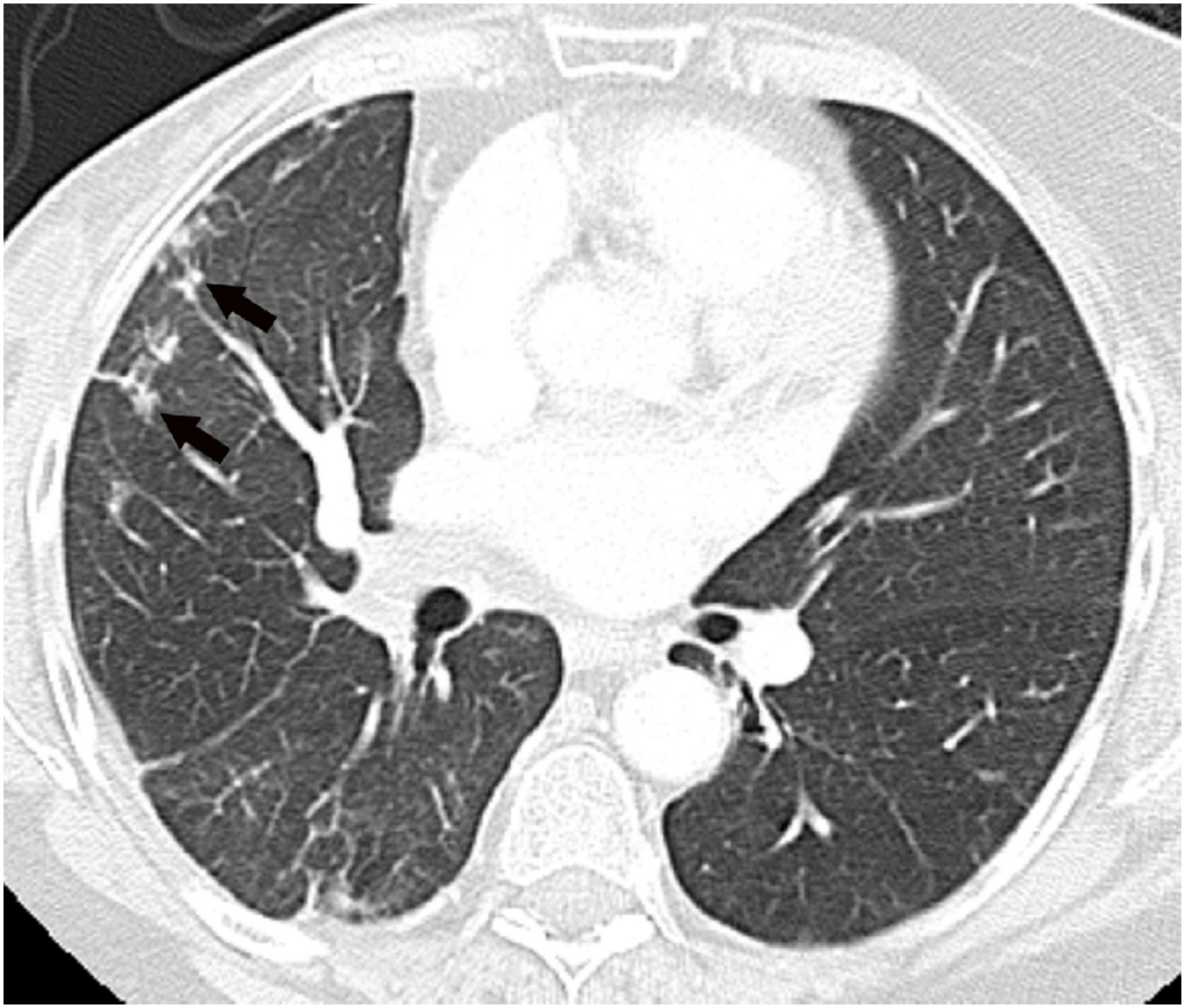

Fig. 11. A 61-year old woman with diagnosis of inflammatory carcinoma of the right breast

(a) Radiotherapy treatment planning field include the right chest wall with medial and lateral tangent fields to a total dose of 51Gy at 1.5Gy per fraction in 34 fractions.

(b) Axial CT image obtained 4 months after treatment ending shows nodular opacities (arrows) included in the irradiated field consistent with nodular-like pattern of radiation pneumonitis.

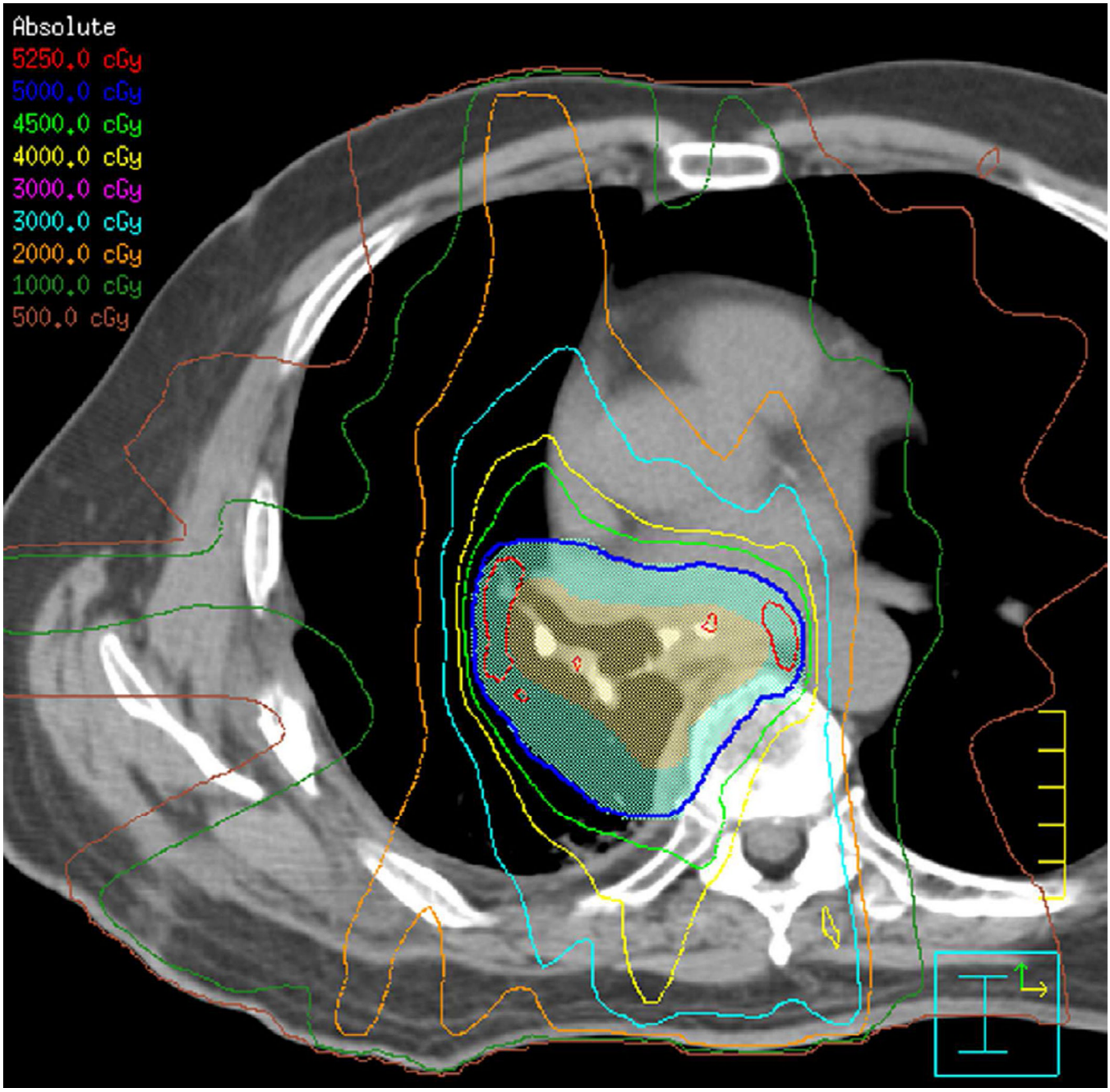

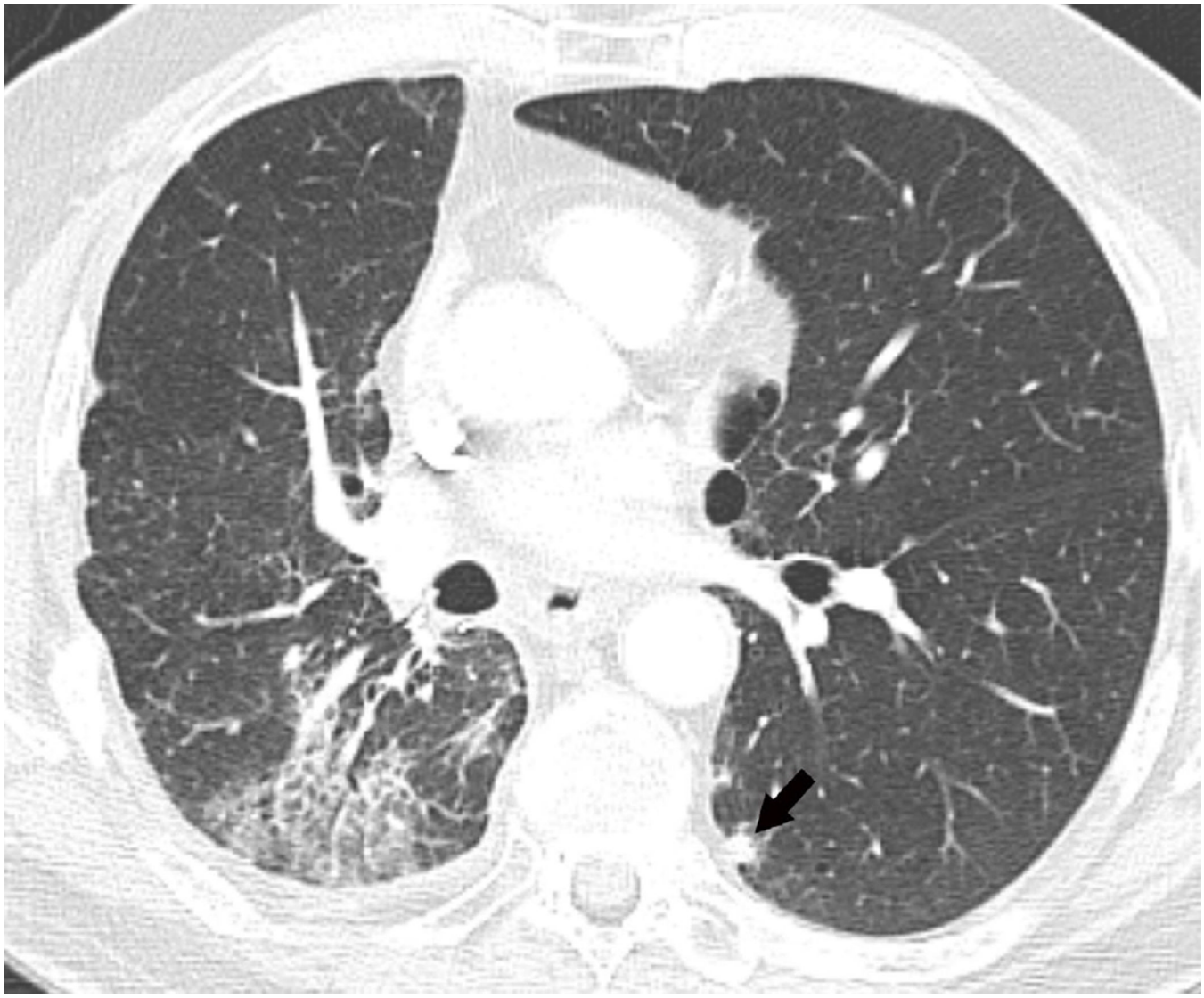

Fig. 12. A 64-year-old man with stage IIIA NSCLC, status post-right lower lobectomy with a positive subcarinal node undergoing post-surgical IMRT

(a) Treatment planning field is situated in the right hilar region and subcarinal nodal regions. Planned treatment dose is 50 Gy at 2 Gy per fraction in 25 fractions.

(b) Axial CT image show nodular lung opacities included in the treatment planning field and consistent with nodular radiation pneumonitis away from the site of the primary tumour (arrow).

(c) Axial CT image demonstrate nodular opacities in the contralateral lung (arrow). Note that although this opacity is included in the irradiated field, iso-dose distribution lines demonstrate that abnormality is included below the 20 Gy area.

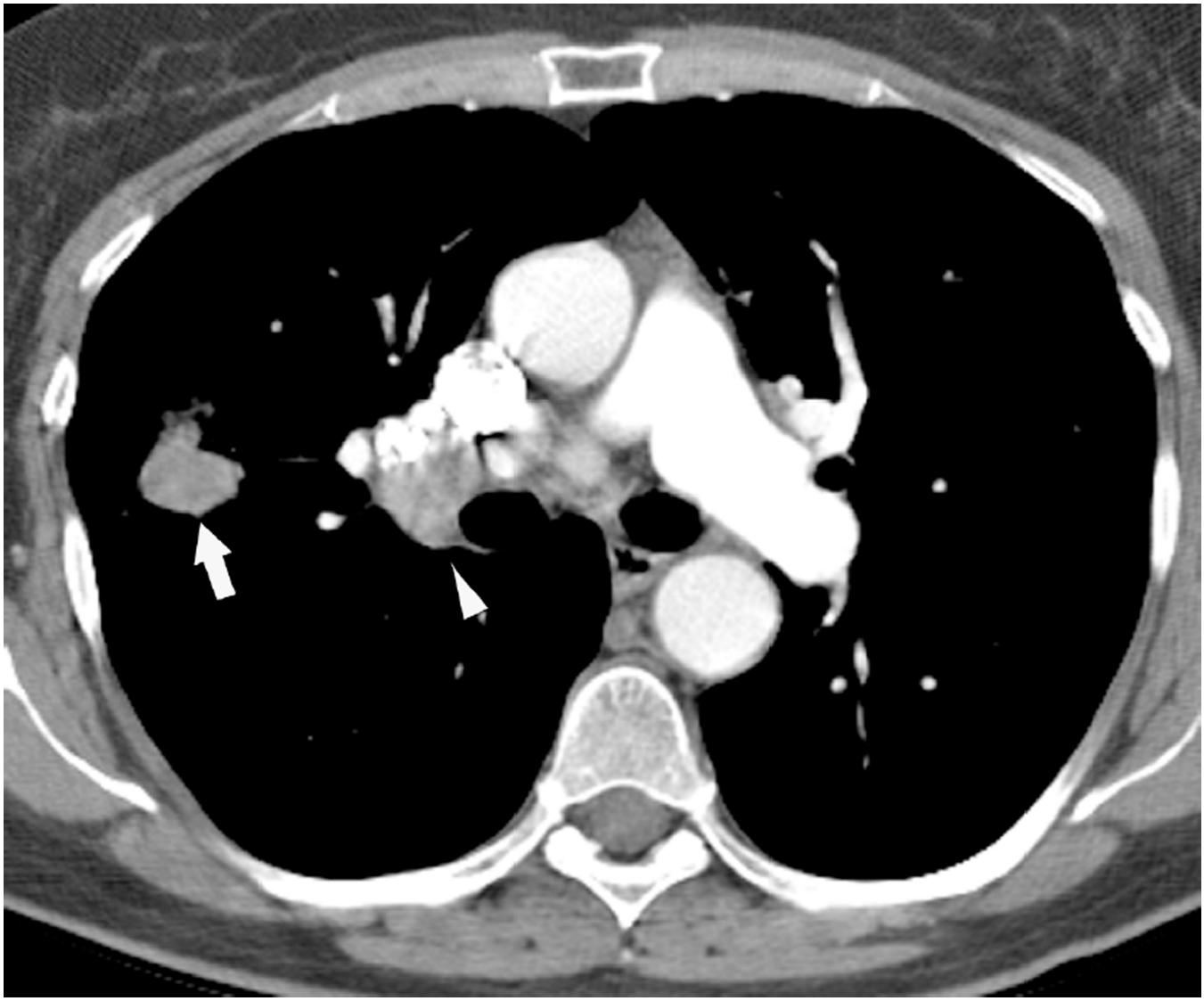

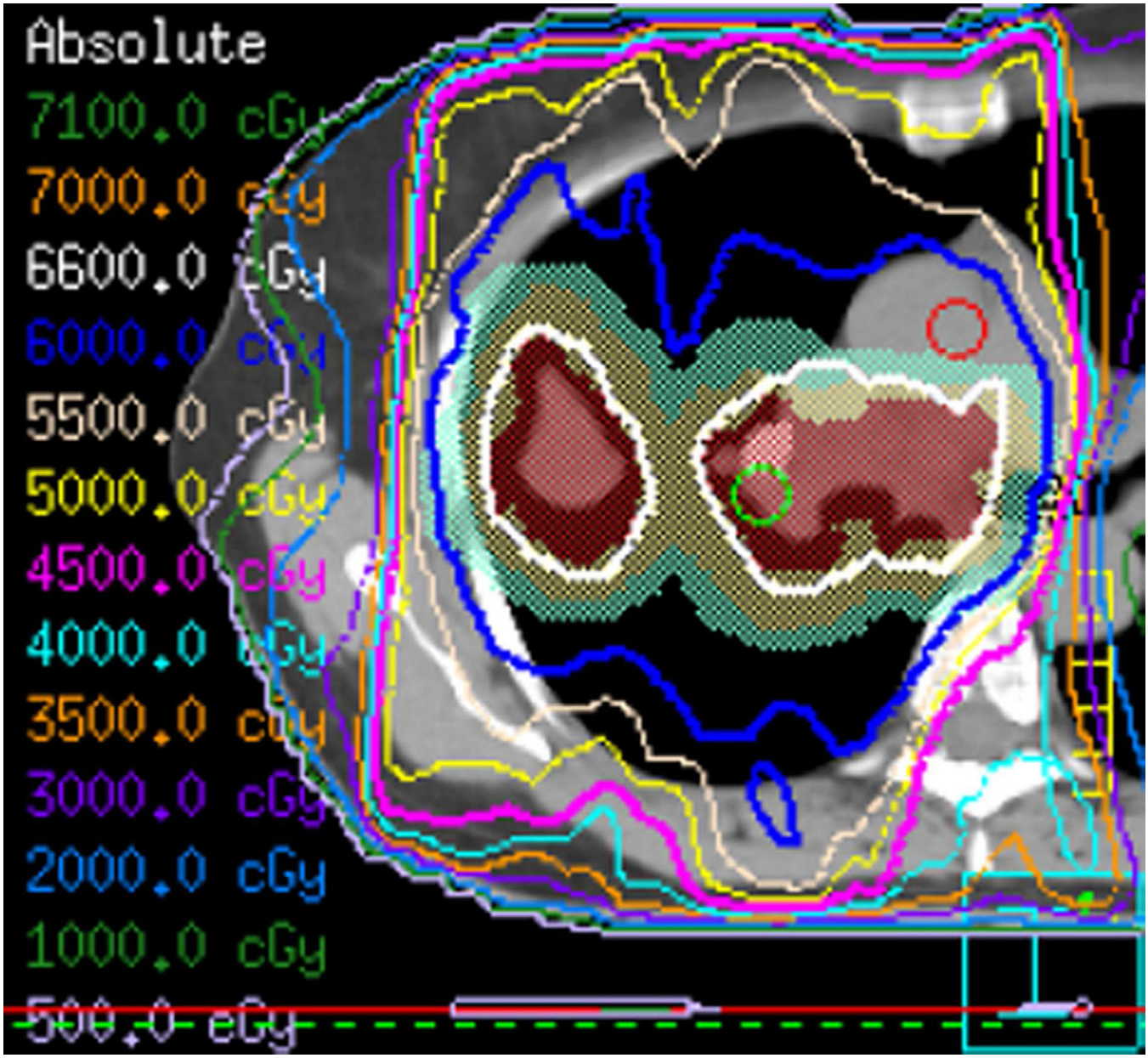

Fig. 13. A 54-year-old woman with a diagnosed stage IIIA right upper lobe NSCLC metastatic to subcarinal and right paratracheal lymph node stations

(a) Axial CT image after administration of intravenous contrast medium and prior to treatment shows a right upper lobe nodule (right arrow) and right hilar adenopathy (white arrowhead) consistent with nodal metastatic disease.

(b) Treatment planning field showing the right upper lobe and mediastinum involvement treated with IMRT in five beams to a total of 60 Gy.

(c) Axial CT image obtained 6 months after treatment ending demonstrate right perihilar consolidative opacities consistent with radiation lung injury (black arrow).

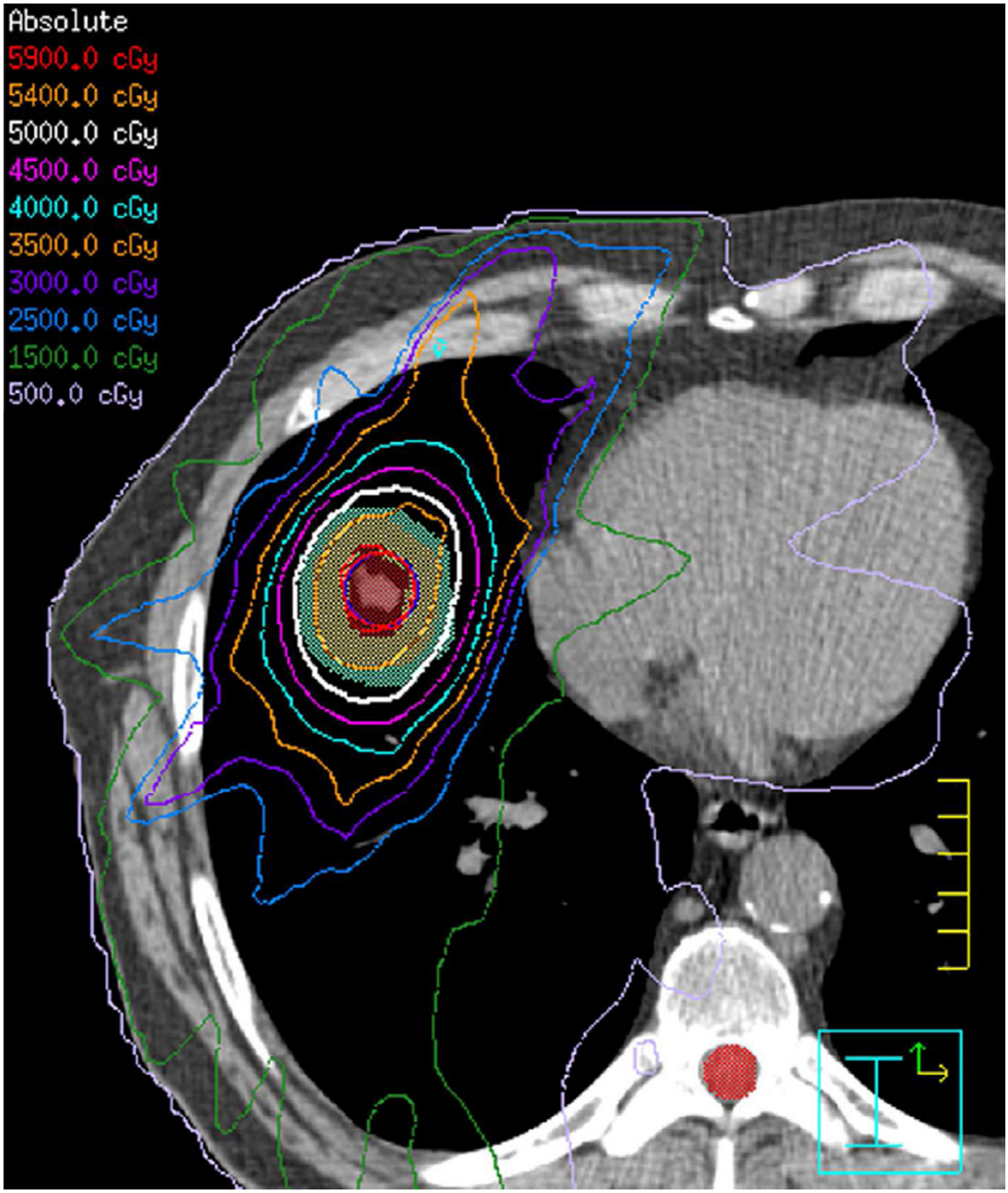

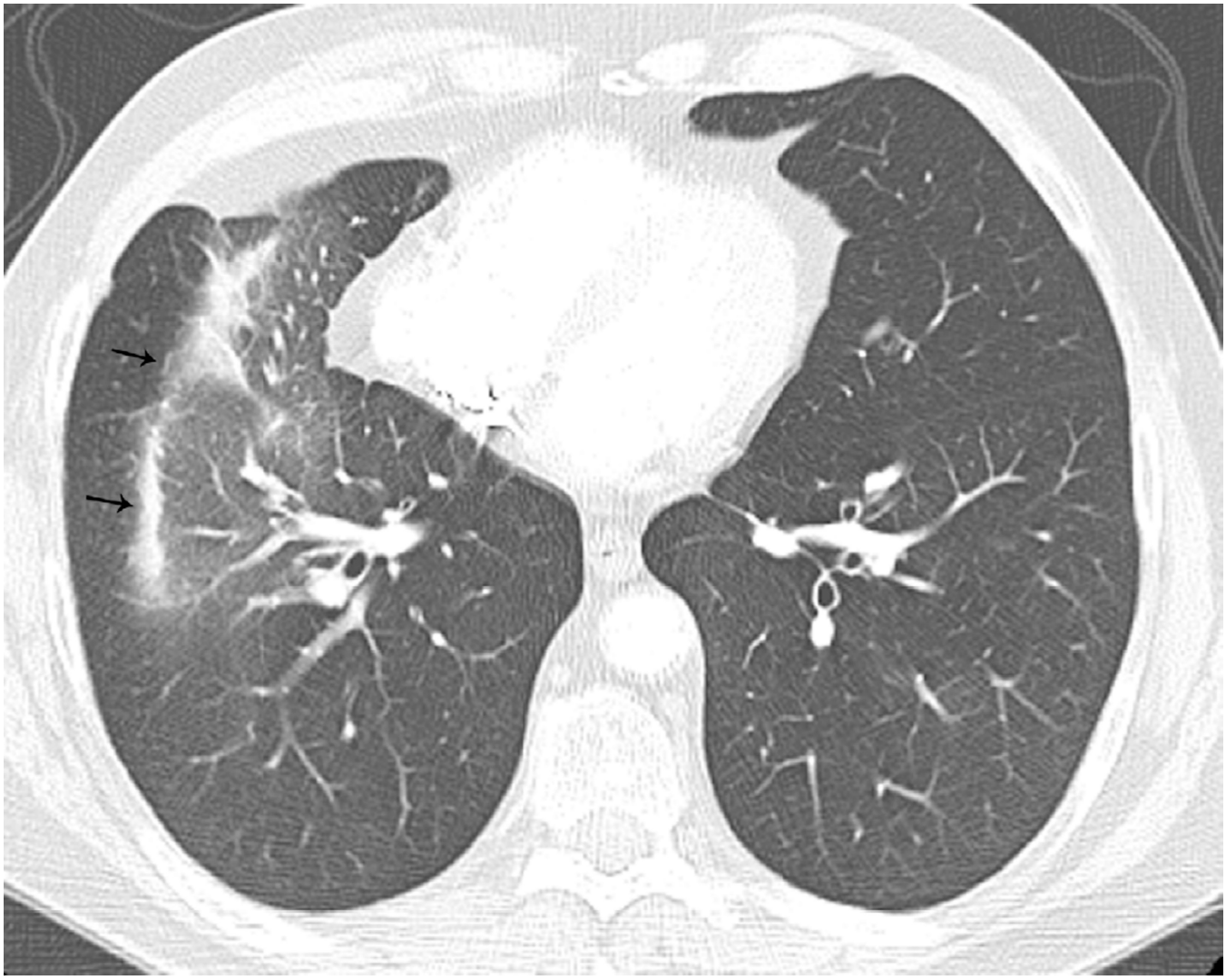

Fig. 14. A 67-year-old man with history of a stage I NSCLC involving the right middle lobe, which was treated with definitive SBRT

(a) Axial CT image obtained prior to treatment demonstrate a 2 cm right middle lobe nodule (arrow).

(b) Treatment planning field for a right middle lobe lung lesion treated definitively to a total dose of 50 Gy in four fractions with a nine-beam stereotactic body radiotherapy plan.

(c) Axial CT image obtained 8 months after completion of therapy shows lung opacities included in the irradiated field (thin arrows). Note that contralateral lung and non-irradiated right lung are spared from lung damage.

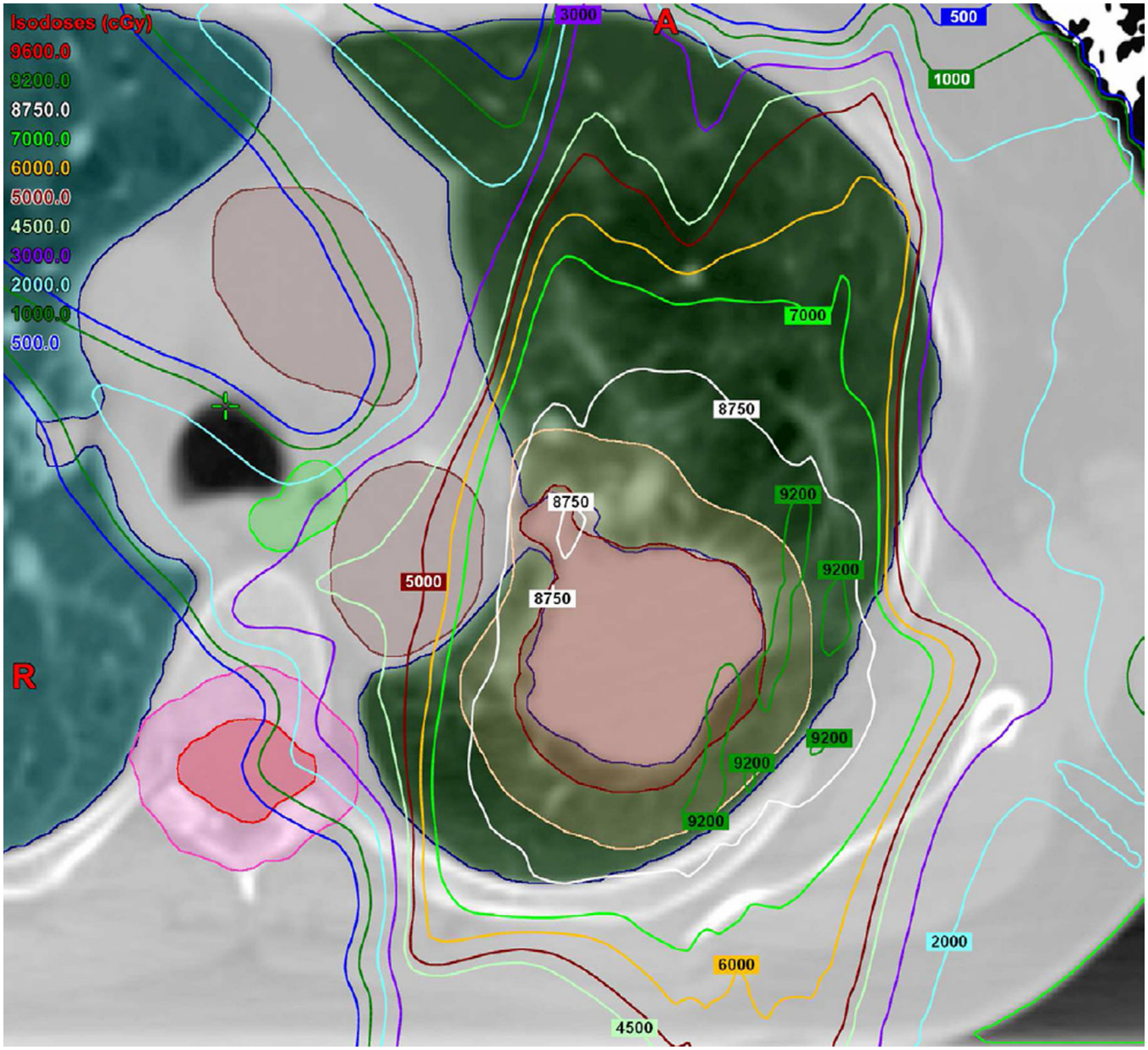

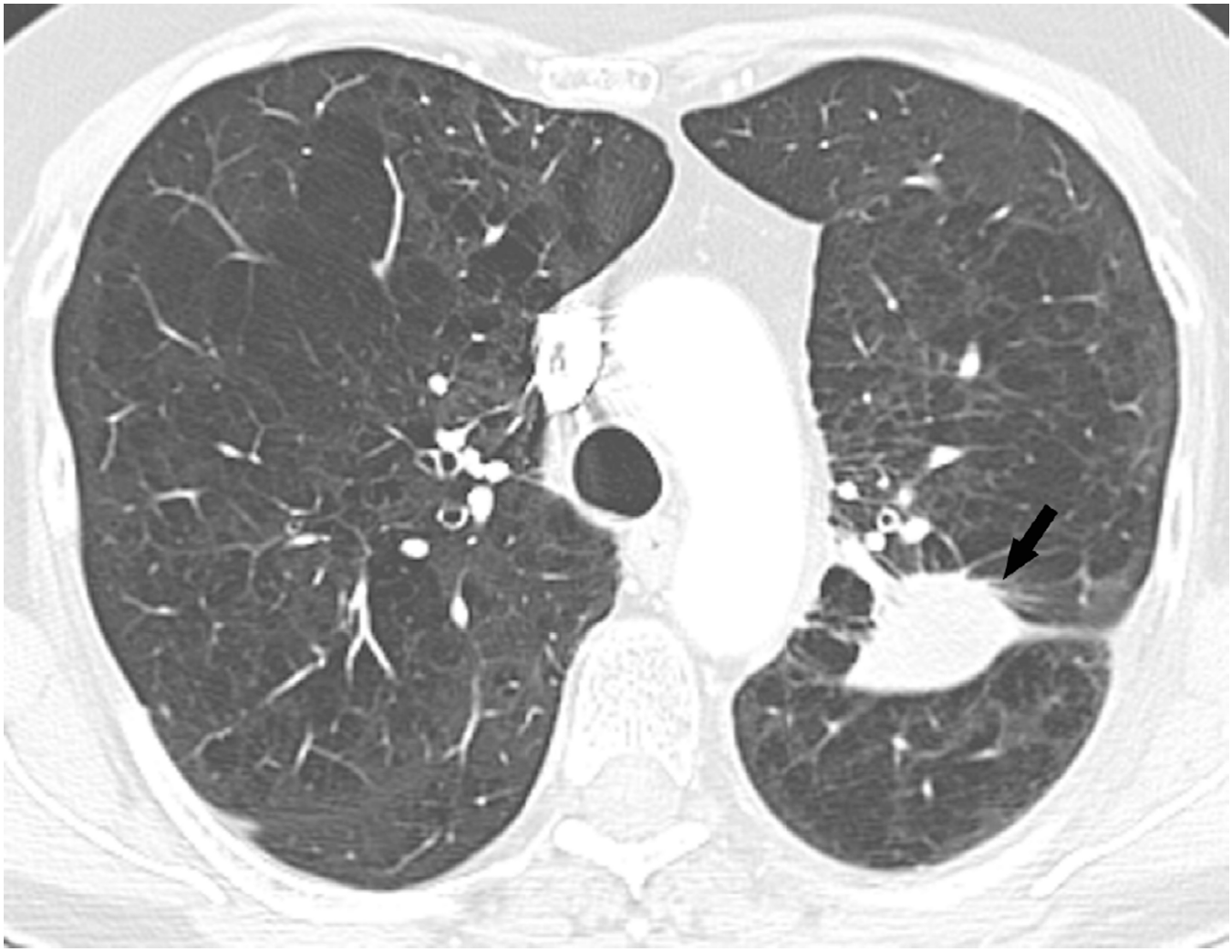

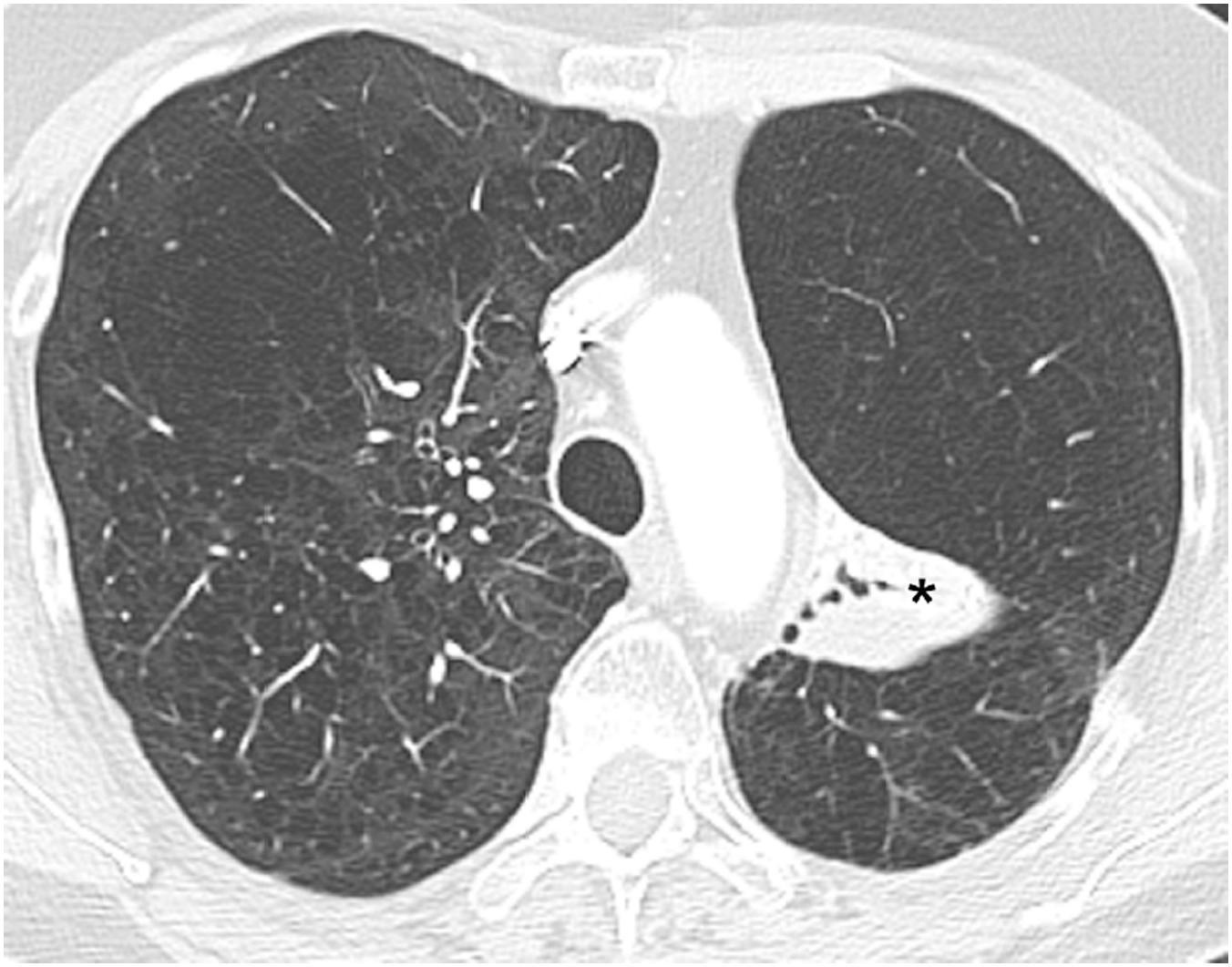

Fig. 15. A 67-year-old woman with a left upper lobe NSCLC. The patient was a poor surgical candidate and was treated with definitive radiotherapy

Proton therapy has been chosen because of the ability to spare normal lung and non-involved mediastinal structures.

(a) Treatment planning field demonstrate three fields using proton therapy. Right posterior oblique, left anterior oblique, and left posterior oblique fields were used with a total dose of 87.5 Co-60 Gy divided over 35 fractions.

(b) Axial CT image 6 months after completion of therapy shows decrease in size of the tumour (arrow).

(c) Axial CT image obtained 18 months after completion of therapy demonstrate left perihilar focal lung opacities with traction bronchiectasis consistent with post-radiation changes (*). Note that remaining lung was spared from radiation damage.